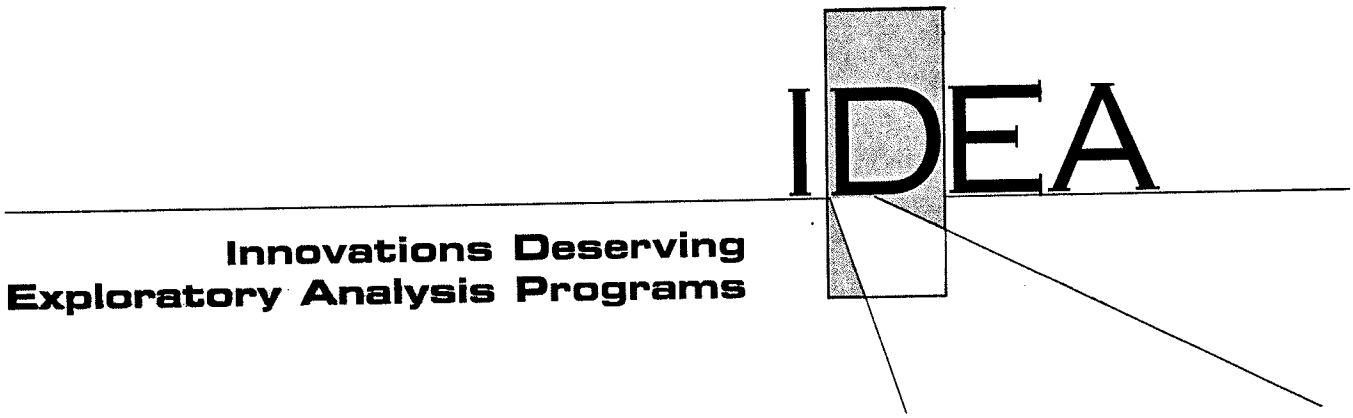

Highway IDEA Program

Development of an Adaptive Damper for Cable Vibration Control

Final Report for NCHRP IDEA Project 92

Prepared by:
C.S. Cai and W.J. Wu, Louisiana State University, Baton Rouge, LA

April 2005

TRANSPORTATION RESEARCH BOARD
OF THE NATIONAL ACADEMIES

INNOVATIONS DESERVING EXPLORATORY ANALYSIS (IDEA) PROGRAMS
MANAGED BY THE TRANSPORTATION RESEARCH BOARD (TRB)

This NCHRP-IDEA investigation was completed as part of the National Cooperative Highway Research Program (NCHRP). The NCHRP-IDEA program is one of the four IDEA programs managed by the Transportation Research Board (TRB) to foster innovations in highway and intermodal surface transportation systems. The other three IDEA program areas are Transit-IDEA, which focuses on products and results for transit practice, in support of the Transit Cooperative Research Program (TCRP), Safety-IDEA, which focuses on motor carrier safety practice, in support of the Federal Motor Carrier Safety Administration and Federal Railroad Administration, and High Speed Rail-IDEA (HSR), which focuses on products and results for high speed rail practice, in support of the Federal Railroad Administration. The four IDEA program areas are integrated to promote the development and testing of nontraditional and innovative concepts, methods, and technologies for surface transportation systems.

For information on the IDEA Program contact IDEA Program, Transportation Research Board, 500 5th Street, N.W., Washington, D.C. 20001 (phone: 202/334-1461, fax: 202/334-3471, http://www.nationalacademies.org/trb/idea)

ACKNOWLEDGEMENTS

The research team is grateful to Dr. Inam Jawed of the NCHRP-IDEA program for awarding this research grant and overseeing its execution.

The research team also appreciates VSL International Ltd for cable material supply, and Lord Corporation, PCB Piezotronics Inc., Dactron Incorporated and Ling Dynamic System Ltd for technical information of their products.

The suggestions and comments from the advisory committee members listed below and the participation of Ph.D. students Marcio Araujo, Xianzhi Liu, and Suren Chen at LSU in the experimental work are also acknowledged.

Advisory Committee Members:

Shashikant Shah, Consultant
Walid Alaywan, Louisiana Department of Transportation and Development
Arturo Aguirre, Federal Highway Administration
Dr. Robert Bruce, Tulane University
Williams B. Conway, Modejeski and Masters, Inc.

TABLE OF CONTENTS

EXECUTIVE SUMMARY

For many cable-stayed bridges in the U.S. and worldwide, large amplitude vibration of cables due to wind-rain induced vibrations has been reported recently. This issue has raised great concerns since excessive cable vibrations will be detrimental to the long-term health of bridges. To address this problem, countermeasures such as changing the cable aerodynamic properties, adding crossing ties/spacers or providing mechanical dampers have been initiated over the years to increase the cable damping.

The goal of this study is to develop the concept of an adjustable Tuned Mass Damper – MagnetoRheological (TMD-MR) damper system that can be adjusted to cope with different external loading conditions. The TMD-MR damper system has two combined advantages. First, as a TMD, the TMD-MR damper system can be attached to any place along the cable. Meanwhile, by using MR fluids, the damping and/or stiffness of the TMD-MR damper system is adjustable. As a result, a high damping efficiency will be achieved by overcoming the drawbacks of the frequency and/or mode sensitivity of the traditional TMD dampers and the position restriction of the traditional MR dampers in cable applications.

Experiments on MR dampers, cable-MR damper system, cable-TMD damper system, and cable-TMD-MR damper system were carried out in the laboratory. MR damper design and dynamic characteristics analysis of the cable-TMD-MR damper system were performed. Major tasks are summarized below.

- Literature about wind-rain induced cable vibration, cable dynamics, cable vibration control, MR fluids and MR dampers were reviewed.
- Performance of two different MR dampers manufactured by Lord Corporation was tested with different loading conditions.
- Basic dynamic characteristics were measured for a 7.16 m steel cable.
- Dynamic characteristics of the cable-MR system were measured to verify the vibration reduction effectiveness of MR dampers to the cable.
- Small size MR dampers were designed and manufactured by the research team since appropriate MR dampers that meet the requirement of the TMD-MR damper system were not commercially available.
- Theoretical discussion on the performance of the cable-TMD-MR damper system was conducted.
- Dynamic characteristics of the cable-TMD-MR damper system were measured to confirm its vibration reduction effectiveness to the cable.

In the conclusion, the research team strongly suggests that the proposed TMD-MR damper system be further studied for field applications on actual cables. This damper system is believed to have addressed the low damping problem of cables practically and cost-effectively. Dynamic characteristics of the cable before and after the installation of dampers should be monitored and compared to verify the damping effectiveness in the field study.

IDEA PRODUCT

This NCHRP-IDEA study has developed the concept of an adjustable Tuned Mass Damper – MagnetoRheological (TMD-MR) damper system and demonstrated the effectiveness of this damper in reducing the cable vibration, regardless of the loading conditions. This adjustable TMD-MR damper has the combined advantages of both TMD dampers and MR dampers. First, a TMD damper can be put any place along the cable, which overcomes the deficiency of conventional mechanical dampers; meanwhile, a MR damper can provide continuously adjustable damping and also it can change the stiffness in a small range, which can help the whole system be effective under different vibration frequencies. As a result, a high damping efficiency can be achieved regardless of both the frequency/mode sensitivity of the TMD dampers and the position restriction of the MR dampers.

CONCEPT AND INNOVATION

Background

As one of the most common but damaging vibration phenomena, wind-rain induced cable vibration has been reported worldwide (Hikami 1986, Matsumoto et al. 1992, Tabatabai and Mehrabi 1999, Main and Jones 2001). Large-amplitude vibrations on the order of 1 to 2 m of stay cables have been observed under certain combinations of light rain and moderate wind speeds of about 10 to 15 m/s. Wind-rain induced cable vibrations can cause fatigue problems and damage cable itself and connections at the bridge deck and towers. This has raised great concerns in the bridge community and has been a cause of deep anxiety for the observing public. According to previous studies, water rivulets on the upper windward surface and the formation of axial flow in the near wake of the cables are believed to be the main causes of wind-rain induced vibrations (Matsumoto et al., 1995).

To address this severe vibration problem, researchers and engineers have been modestly successful by trial-and-error methods to increase the cable damping, such as by treating cable surface in order to improve its aerodynamic properties (Flamand 1995, Phelan et al. 2002), adding crossing ties/spacers (Langsoe and Larsen 1987) or providing mechanical dampers (Tabatabai and Mehrabi 2000).

Mechanical dampers have been proven a useful method to reduce cable vibration. However, the reduction effect is not optimal since the traditional mechanical dampers need to be installed close to the lower end of cables. TMDs can overcome this restriction and they were experimentally investigated and recommended for cable vibration reduction (Tabatabai and Mehrabi 1999). However, this recommendation was based on

the observed damping effect of TMD dampers on the free vibration of a cable in the first mode. It has been found that the wind-rain cable vibrations are often related to higher mode vibrations. Therefore, A TMD designed for the first mode vibration is most likely not effective for higher mode vibrations since the TMD effectiveness is frequency/mode sensitive.

Objectives

The objective of this study is to develop the concept of an adjustable TMD-MR damper system that can be adjusted to deal with different cable vibrations, regardless of the cable vibration frequency/mode. The adjustable TMD-MR damper system will be designed using controllable MR fluids.

INVESTIGATION

Investigation Approach

As an important step of this study, a literature review was carried out in the area of MR dampers, wind-rain induced cable vibration, cable dynamic characteristics and other related topics.

To fully understand the dynamic characteristics of cable system with attached TMD-MR dampers and for comparison consideration, it is very important to investigate first the individual MR damper, pure cable dynamic properties, cable dynamic properties with a TMD, and cable dynamic properties with a MR damper. Since no available commercial MR dampers can match the experimental requirements, the investigation group designed and manufactured two types of MR dampers. One of them was discarded because of its maintenance problem. Several scaled-down prototypes of the second design were manufactured with different sizes and one was chosen for the TMD-MR damper system. Finally, under the guidance of some preliminary theoretical results, dynamic characteristics of the cable system with the TMD-MR damper hung on the cable were investigated experimentally.

Investigation of Individual MR Dampers

MR controllable fluids are among those new materials introduced into civil engineering applications in recent years. MR fluids typically consist of micron-sized,

magnetically polarizable particles dispersed in a carrier medium such as water, mineral or silicone oil. An essential characteristic of MR controllable fluids is their ability to reversibly change from a free-flowing, linear viscous fluid to a semi-solid with controllable yield strength in milliseconds when exposed to a magnetic field. MR fluids appear to be attractive for civil engineering applications in controllable fluid dampers because their large output forces, stable performance to temperature variations and impurities, low power supply requirement, and quick response (Carlson 1994, Carlson and Weiss 1994, Carlson et al. 1995).

Though the researches and applications of MR dampers have attracted much attention in civil engineering community, the main previous effort focuses on structures control under seismic excitation. To the investigators' knowledge, there are just a few publications and online resources about the use of MR dampers to reduce the cable vibrations (Johnson 1999a and 1999b, Lou et al. 2000, Christenson 2002). The Dongting Lake Bridge that was built two years ago in China is the first application of MR dampers for cable vibration control. There is an ongoing similar application for Sutong Bridge over the Yangtze River in China (Lord Corporation, 2004). The Sutong Bridge will be the longest cable stayed bridge in the world with a span length of 1088 m.

Two models of MR dampers from Lord Corporation were tested to obtain their performance curves before they were used to reduce cable vibration. Some relative parameters provided by the company are listed in Table 1. Experiments on the RD-1097-01 MR damper are presented in detail because its output damping force is more suitable for the present cable application than RD-1005-3.

Table 1: Basic Data for MR damper from Lord Corporation

	RD-1005-3	RD-1097-01
Maximum Extension (mm)	53	58
Body Diameter (mm)	41	32
Weight (N)	8	5
Electrical Characteristics:		
Input Current (continuous)	1 amps maximum	0.5 amps maximum
Input Current (intermittent)	2 amps maximum	1.0 amps maximum
Damper Force:		
2 in/sec at 1 amp	>2224 N	>98 N
8 in/sec at 0 amp	<667 N	<9 N

A Universal Test Machine (UTM) 5P was used to investigate the two dampers as shown in Photograph 1. This machine has a maximum output force of 5kN. Dampers were tested vertically in the machine frame using a displacement control method with amplitude of 10mm or 5mm. The force and displacement time series data were read by the computer controlled data acquisition system every 0.01 or 0.02 seconds. Generally, experiments stopped automatically after 20 cycles. The velocity of the MR damper was obtained from the displacement with a forward-difference approximation. An ampere meter and a Wonder Box device controller were connected in series with the MR damper to measure and adjust the current in the MR damper. Different experimental parameters were considered including different working temperatures, loading wave types, loading frequencies and currents provided to the MR dampers.

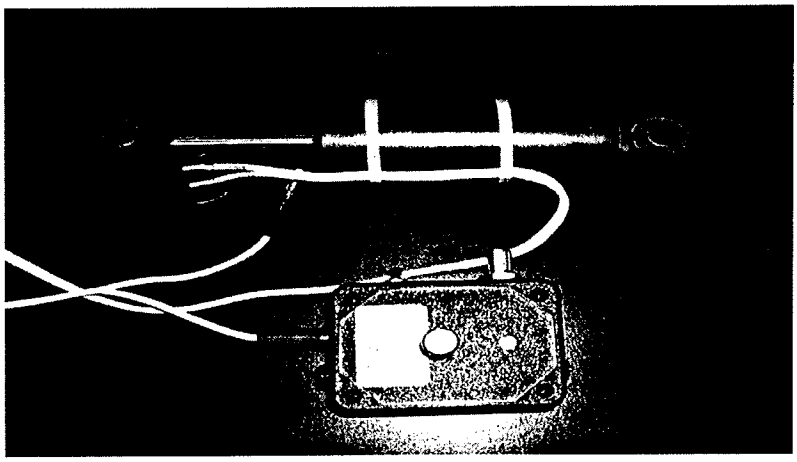

(a) Damper and Wonder Box Device Controller

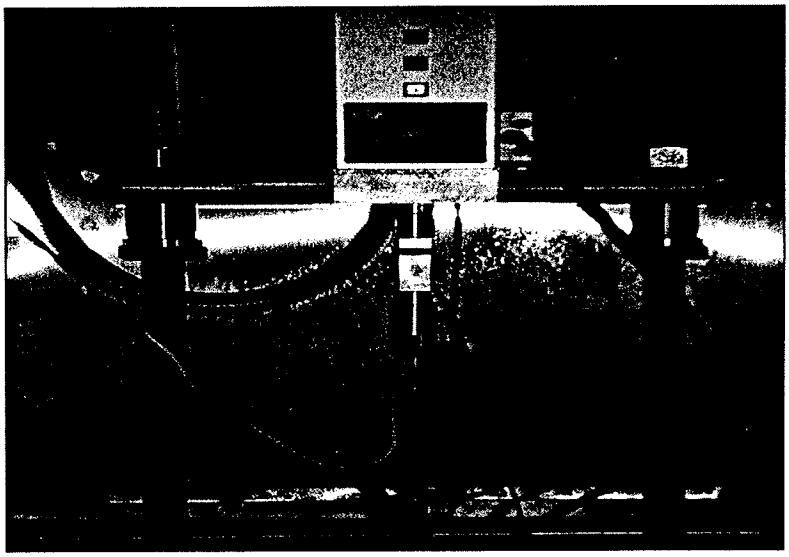

(b) RD-1005-3 in Loading Frame

Photograph 1: Damper and Loading Set-up

MR Damper Performance with Different Currents

Effects of electric currents inside the MR damper on the damper performance are discussed in this part. Eight current levels were considered as 0A, 0.05A, 0.1A, 0.15A, 0.2A, 0.3A, 0.4A and 0.5A. Presented here are some typical performance curves under a sine-loading wave with a constant loading frequency of 1Hz, amplitude of 10mm, and an experiment temperature of 20°C.

From Fig. 1(a), we can observe that the maximum output damping force is about 10N with a current of 0A, which is called passive mode of the MR damper, and about 80N when the current increases to 0.50A. Therefore, the ratio between the peak output damping force at the maximum current to the one at passive mode, or called the dynamic range of the MR damper, is 8. Fig. 1(b) shows that the curve of displacement versus output damping force is almost a rectangle. From the point of view of energy dissipation, the larger displacement-force curve loop can dissipate more energy since the area of the loop represents the energy dissipated in each cycle. Therefore, with a larger current, the MR damper can dissipate more energy for each cycle. According to Fig. 1(c), the curve of the velocity versus the output damping force can be roughly expressed with some piecewise linear functions. From Fig. 1(d), the relationship curve between the displacement and velocity is almost an ellipse, as we expected. The relationship between the maximum output damping force and the current input is plotted in Fig. 2.

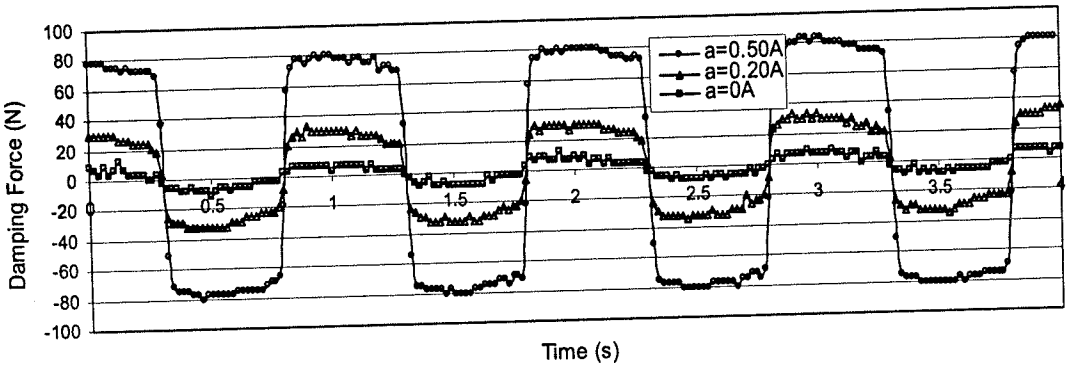

(a) Damping Force Time Series

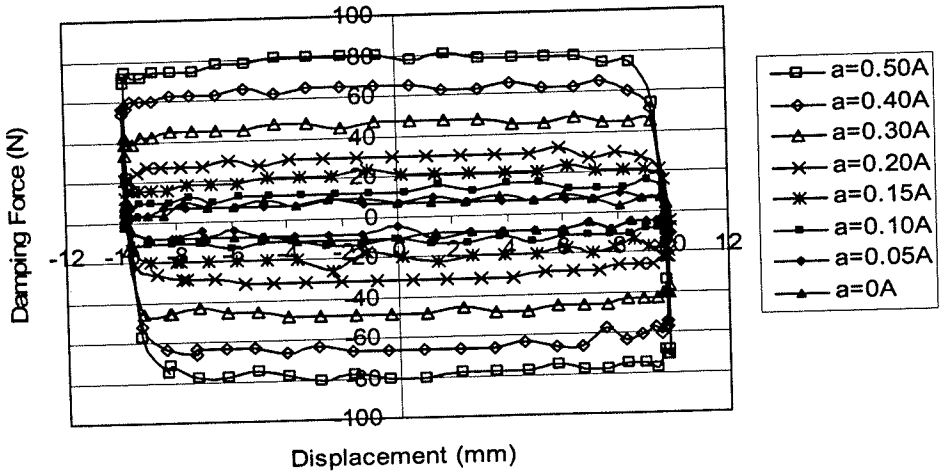

(b) Damping Force versus Displacement

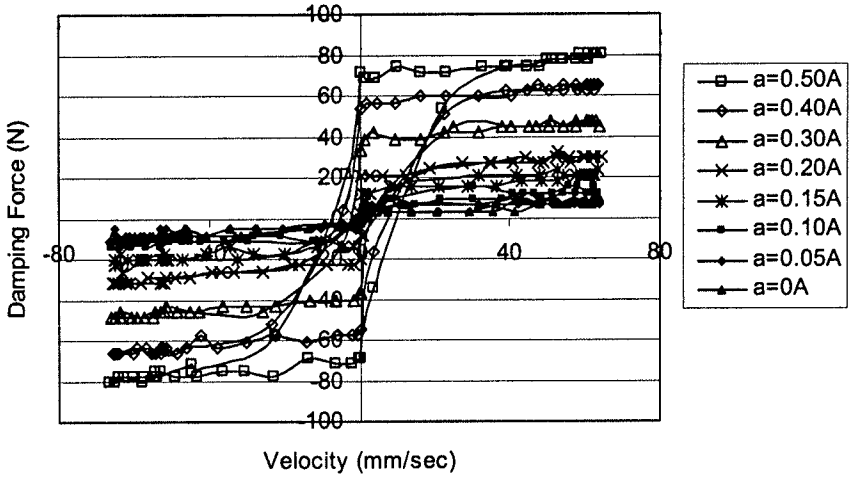

(c) Damping Force versus Velocity

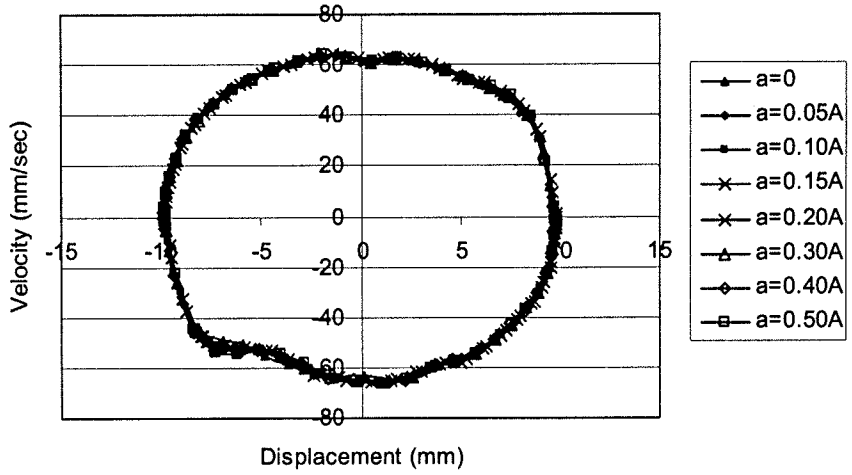

(d) Velocity versus Displacement

Fig. 1: Performance Curve of MR Damper with Different Current

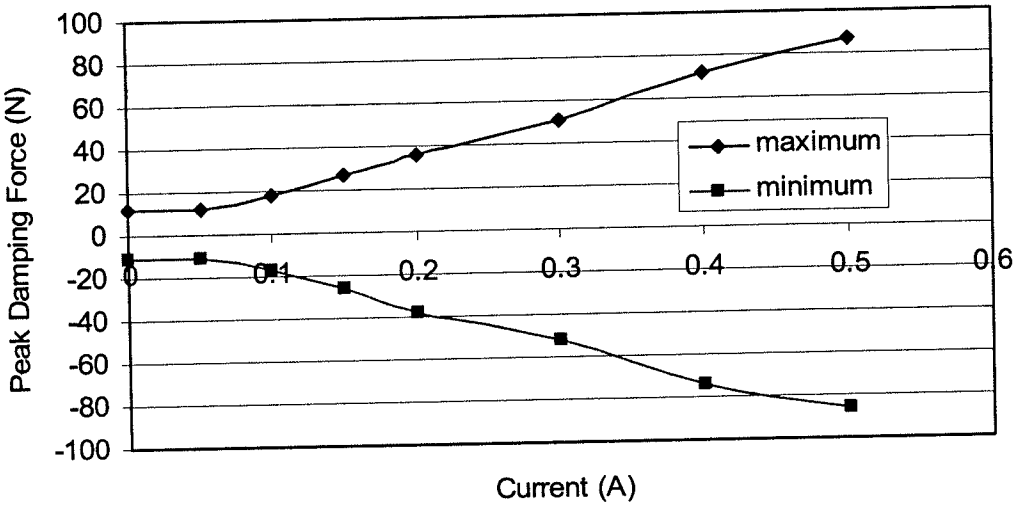

Fig. 2: Peak Output Damping Force versus Current

MR Damper Performance with Different Frequencies

Effects of the loading frequencies on the damper performance are discussed in this part. Five loading frequencies are chosen as 0.5, 1, 2, 2.5 and 5Hz. The currents inside the MR damper chosen to discuss are indicated in the following figures. All the other parameters are the same as in the previous section. In the following figures, "D" means displacement, "F" means output damping force, and "V" means velocity.

It can be observed from Fig. 3 that with the increase of the current, the effect of loading frequency on the output damping force-displacement relationship decreases. However, as shown in Fig. 4, the damping force-velocity relationship is more sensitive to the loading frequency.

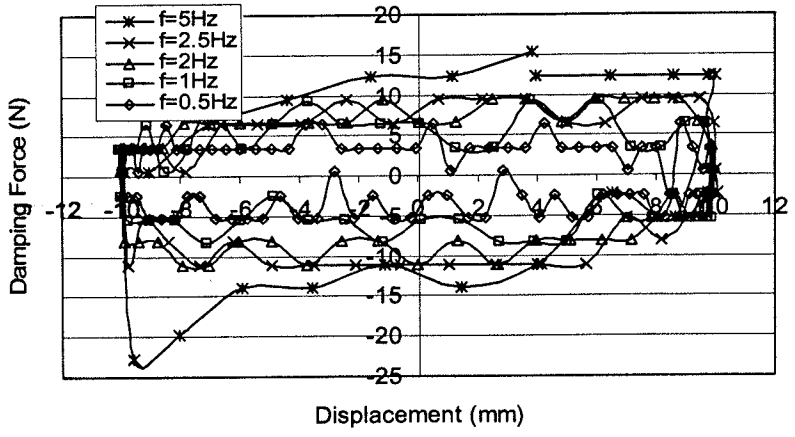

(a) 0A Current

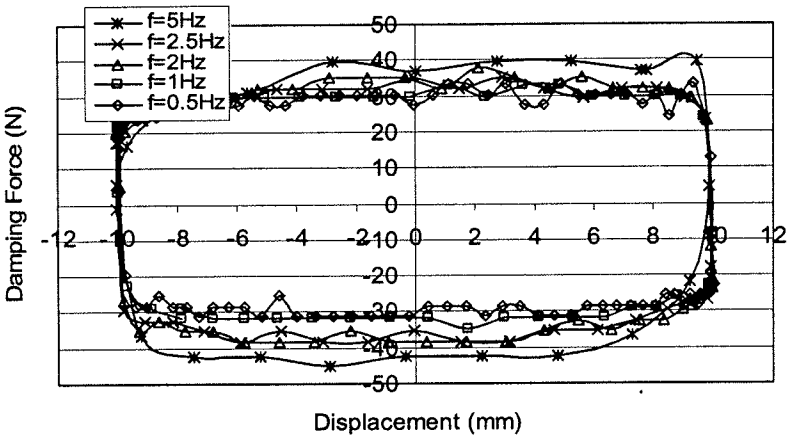

(b) 0.2A Current

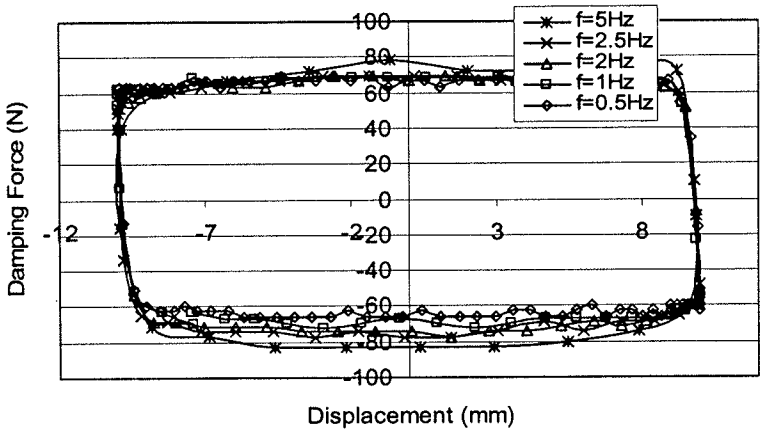

(c) 0.4A Current

Fig. 3: D-F Curve with Different Frequency at Constant Current: (a) 0A, (b) 0.20A, (c) 0.40A

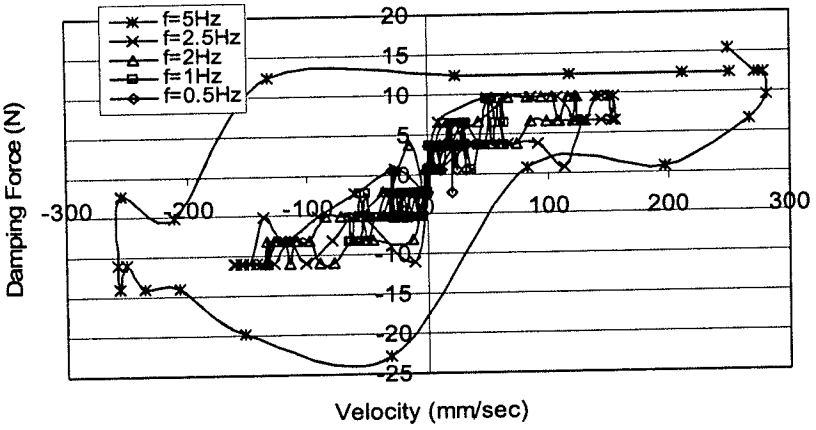

(a) 0A Current

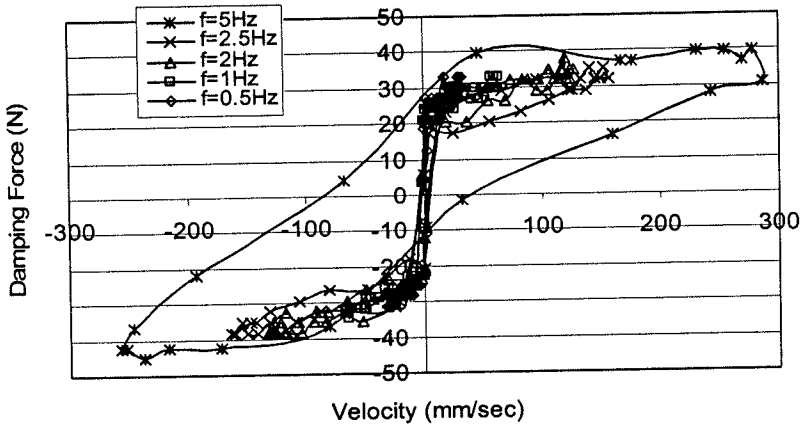

(b) 0.2A Current

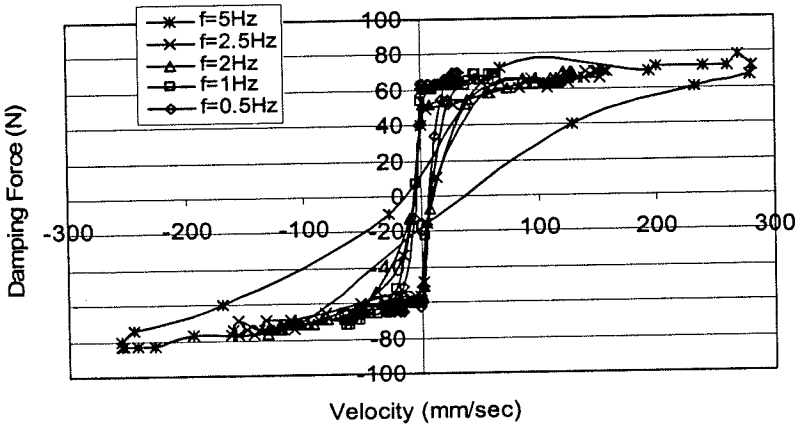

(c) 0.4A Current

Fig. 4: V-F Curve with Different Frequency at Constant Current: (a) 0A, (b) 0.20A, (c) 0.40A

MR Damper Performance with Different Loading Waves

Effects of loading types (simulated using different loading waves) on the damper performance are discussed in this part. Three loading waves are chosen as sine, triangle and pulse waves as shown in Fig. 5(a). All the other experimental parameters are the same as in the previous section, unless specified differently. In the following figures, the current is 0.4A and the loading frequency is 1Hz.

We can observe from Fig. 5(b) that the corresponding output damping force of the triangle-loading wave is less than that of the sine-loading wave. For the pulse-loading wave, the output damping force is also in the form of a pulse wave. From Fig. 5(c), we can observe that, in the case of the pulse-loading wave, the displacement-force curve is a curved quadrangle that is much smaller than the rectangular curves of the other two loading cases. Since the peak velocity of the pulse-loading wave is much larger than (and is thus out of range of) the other two cases, the corresponding curve of the pulse-loading wave is not plotted in Fig. 5(d) and 5(e). From these two figures, it can be observed that the velocity-force curve of the sine-loading wave is flatter than that of the triangle-loading wave. The ellipse displacement-velocity curve loop for the sine-loading wave is larger than that of the triangle-loading wave.

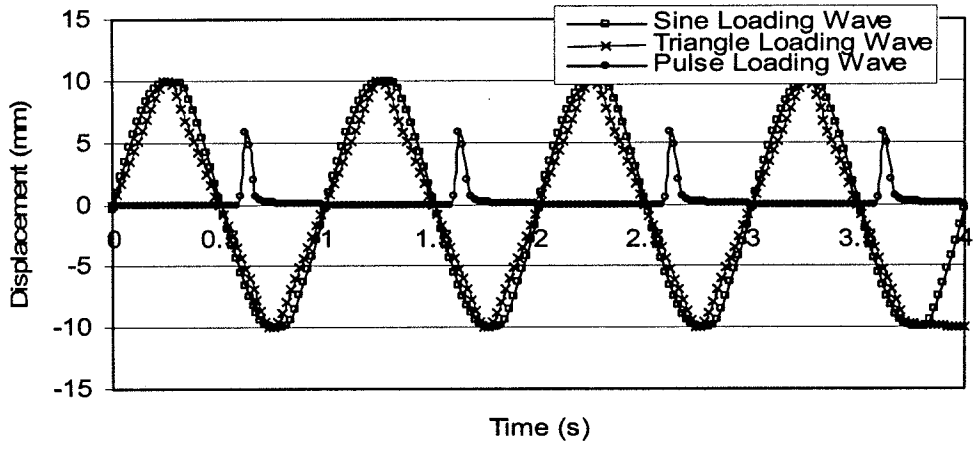

(a) Displacement Time

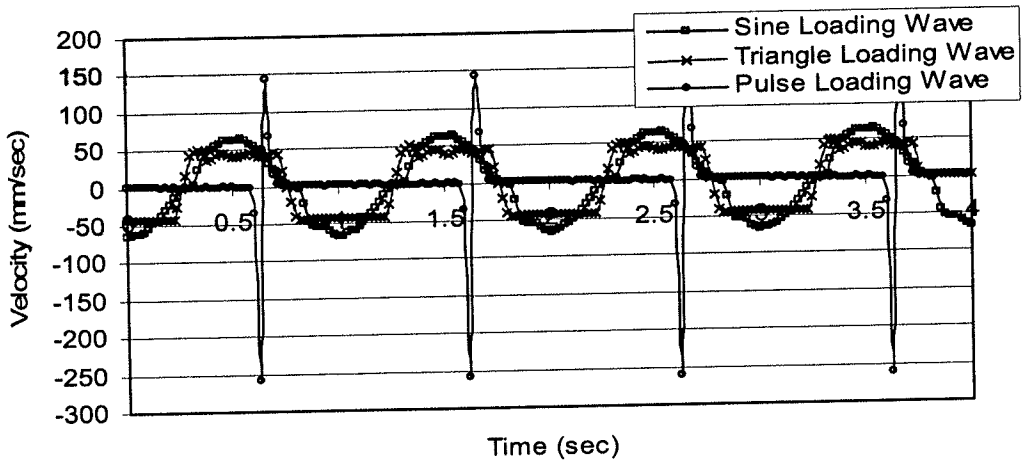

(b) Damping Force Time Series

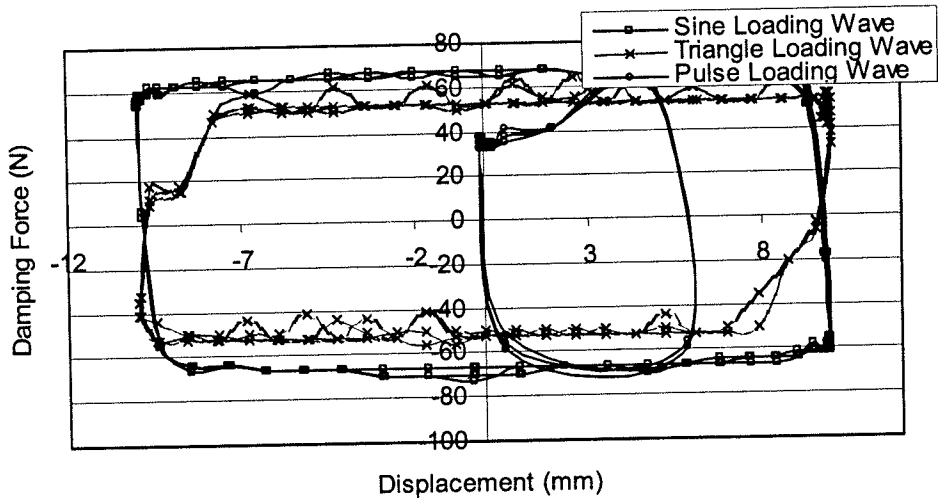

(c) Damping Force versus Displacement

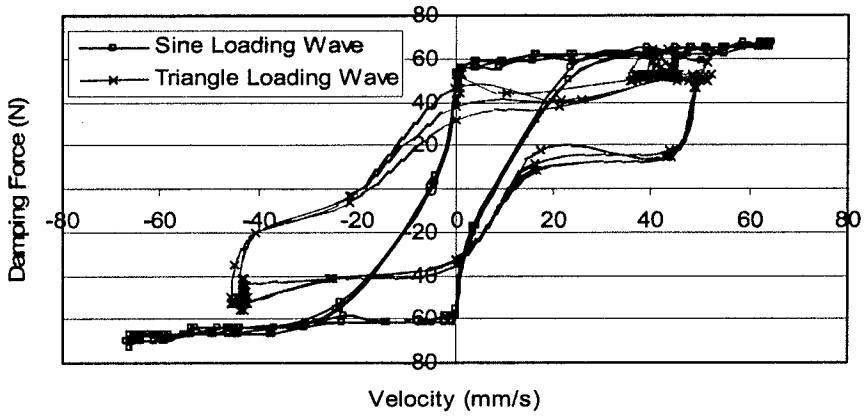

(d) Damping Force versus Velocity

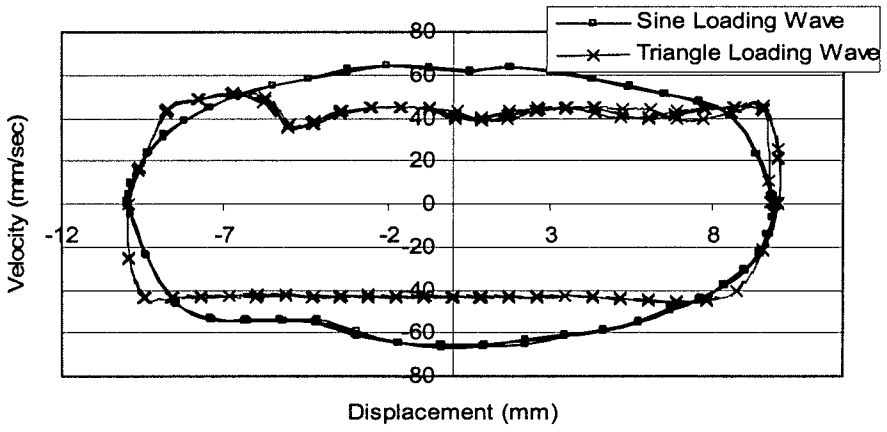

(e) Velocity versus Displacement

Fig. 5: Performance Curve with Different Loading Waves

MR Damper Performance with Different Temperatures

Effects of working temperatures on the damper performance are discussed in this part. The experimental temperatures were set to 0°C, 10°C, 20°C, 30°C, 40°C and 50°C. The currents and frequencies were varied the same way as in the previous tests. Only the sine-loading wave was investigated.

We can observe from Fig. 6 that temperature does have some effect on the performance curve of the MR damper. With the increase of the temperature, the output damping force decreases nonlinearly. The damping force-displacement curves of temperatures at 0°C, 10°C and 20°C cluster into one group and the other three cases, 30°C, 40°C and 50°C into another group. Similar observations can be made from the velocity-force curves as shown in Fig. 7, but not as obvious as that in Fig. 6. More experimental results are given in Appendix A.

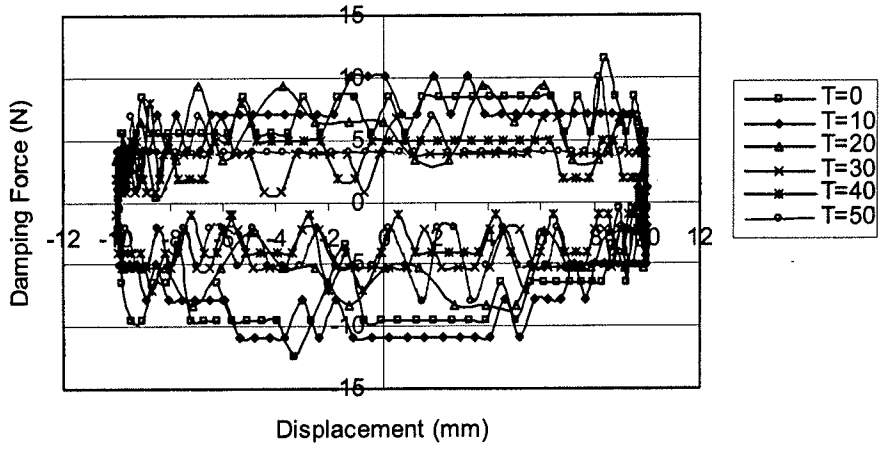

(a) 0A Current

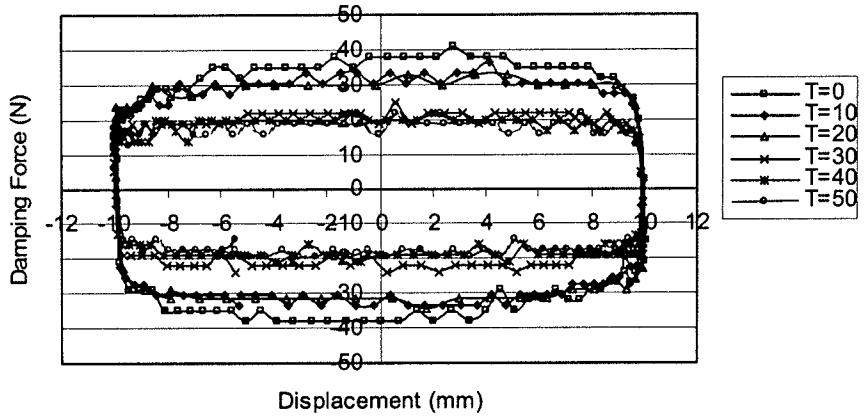

(b) 0.2A Current

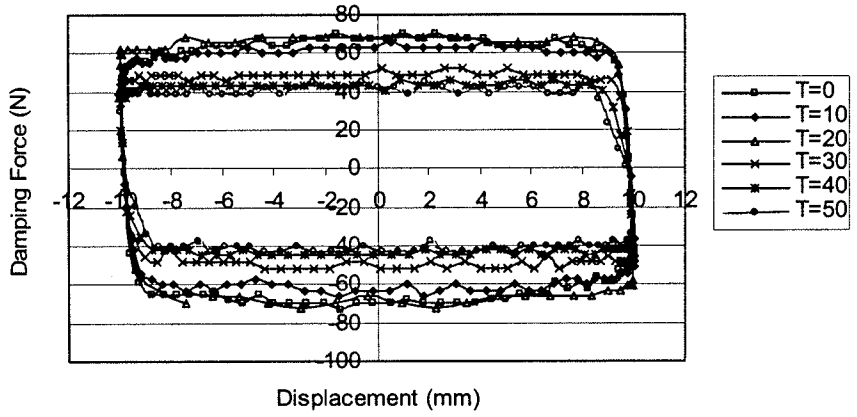

(c) 0.4A Current

Fig. 6: D-F Curve with Different Temperature: (a) 0A; (b) 0.2A; (c) 0.4A

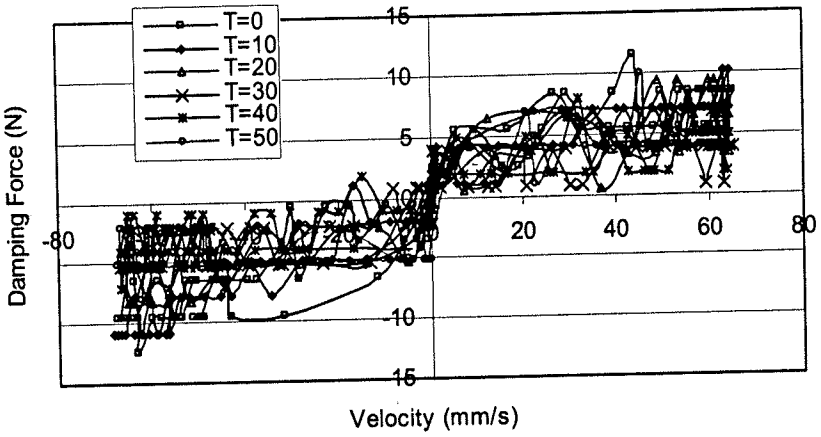

(a) 0A Current

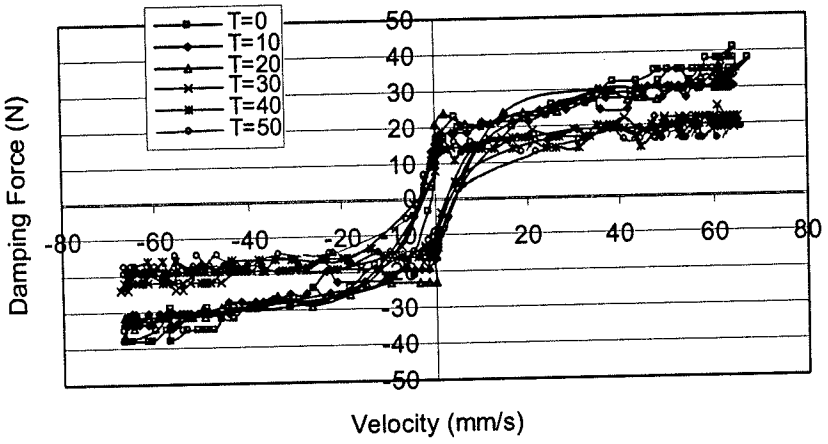

(b) 0.2A Current

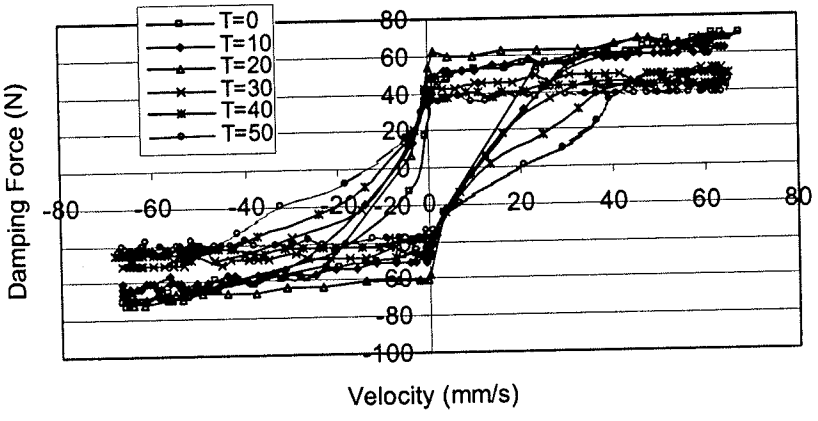

(c) 0.4A Current

Fig. 7: V-F Curve with Different Temperature: (a) 0A; (b) 0.2A; (c) 0.4A

Cable Vibration Control with MR Dampers

Scaling Theory for Model Cable

Generally speaking, scaling factors should be decided based on scaling principles to maintain the similarities between the prototype cable and the test model. However, it is not entirely possible to achieve these similarities for all the parameters. Several different scaling criteria have been proposed for model experiments in the literature. Since there is a wide range of actual cable parameters, and there is no particular prototype in this investigation, we just need to verify that the corresponding prototype stay cable is not too abnormal from the "averaged" value. As stated in Tabatabai and Mehrabi's (1999) report, the average length and outside diameter of cables in their database are 128 and 0.182 meters. The minimum, maximum, and average inclination angles are 19, 82, and 38 degrees, respectively. The minimum and average first mode frequencies are approximately 0.26Hz and 1.15Hz, respectively. The scaling criterion used here is pretty much the same as that of Tabatabai and Mehrabi's (1999), meaning that the scaling factor for velocity between the prototype and the model is 1 and for the length dimension is n, namely 8 in the present study. Based on these two scaling factors, scaling factors for other associated parameters can be calculated by physical relationships. Table 2 provides information for the model cable parameters used in the present experimental studies. Parameters for the corresponding prototype cable can be calculated using Tables 2 and 3.

Table 2: Typical Model Parameters

Frame Distance (l)	7.0 m	Frame Height (h)	1.40 m
Cable Length (L)	7.16 m	Cable Angle (α)	11.27°
Cable Area (A)	98.7 mm^2	Axial Stress (σ)	162.7 Mpa
Cable Number (N)	1	Axial Force (T)*	16064.5 N

*: These parameters may change according to different experiments.

Table 3: Dynamic Scaling Relationships (Tabatabai and Mehrabi, 1999)

Parameter	Scaling factor (model/ prototype)
Dimension	1/n
Area	$1/n^2$
Volume	$1/n^3$
Young's Modulus	1
Material Strength	1
Density	1
Poisson's Ratio	1
Damping Ratio	1
Spring Constant	1/n
Mass	$1/n^3$
Signal Frequency	n
Dynamic Time	1/n
Displacement	1/n
Velocity	1
Acceleration	n
Stress	1
Strain	1
Force	$1/n^2$
Energy	$1/n^3$

Test Setup and Equipments

Fig. 8 shows the setup of the cable model system. The one strand steel stay cable is composed of seven wires with a cross section of 98.7mm^2. Both ends of the cable are anchored to the frame with different heights and the two ends can be considered as fixed. Since the lower end goes though a hydraulic jack before it is anchored, an adjustable tension force can be put on the cable. Nine tension forces are chosen to measure the vibration control effect of the added MR damper under different tension forces. The geometric relation of some specific points is shown in the figure. As indicated in the figure, point D is the middle point, B and F are the 1/4th points, and C and E are the other two 1/3rd points of the stretched cable. Those points are installation positions for external vibration loadings, the damping device and the measuring sensors.

Photographs 2 through 7 show the equipments used in the experiment studies. V408 vibrator and PA100E CE amplifier purchased from Ling Dynamic Systems Ltd were used to generate and amplify the forced vibration. Hydraulic jack was used to provide axial tension force. PCB model 352C22 accelerometers and model 480B21 signal conditioner purchased from PCB Piezotronics Inc., and Photon data acquisition from Dactron Incorporated were used to measure, amplify and acquire the acceleration signals, respectively. Photograph 8 shows the damper connected to the cable.

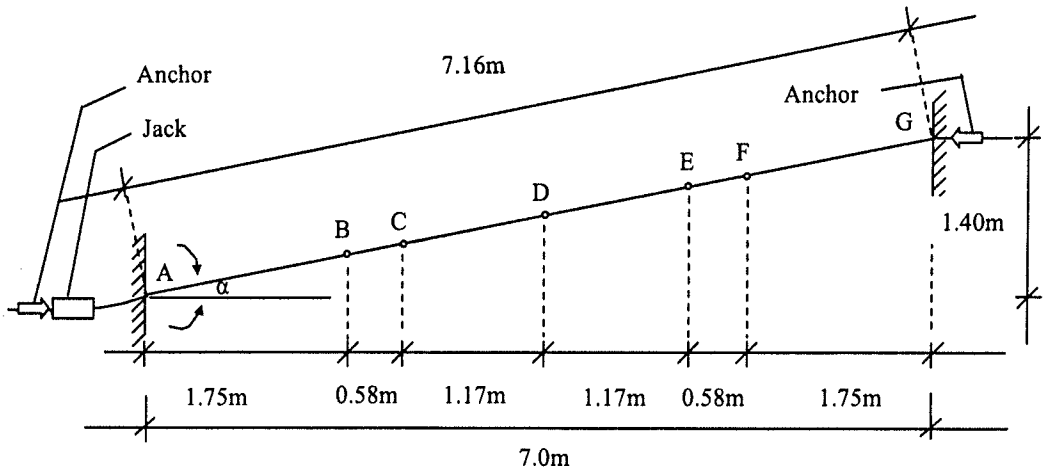

Fig. 8: Experimental Cable Setup

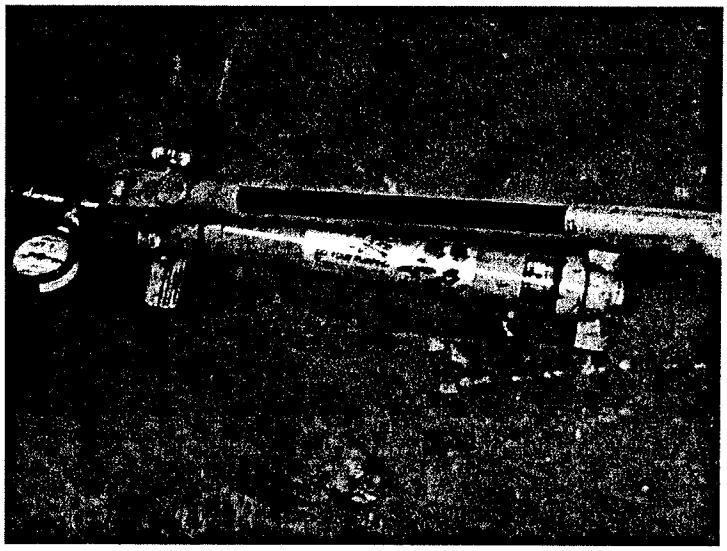

Photograph 2: Hydraulic Jack

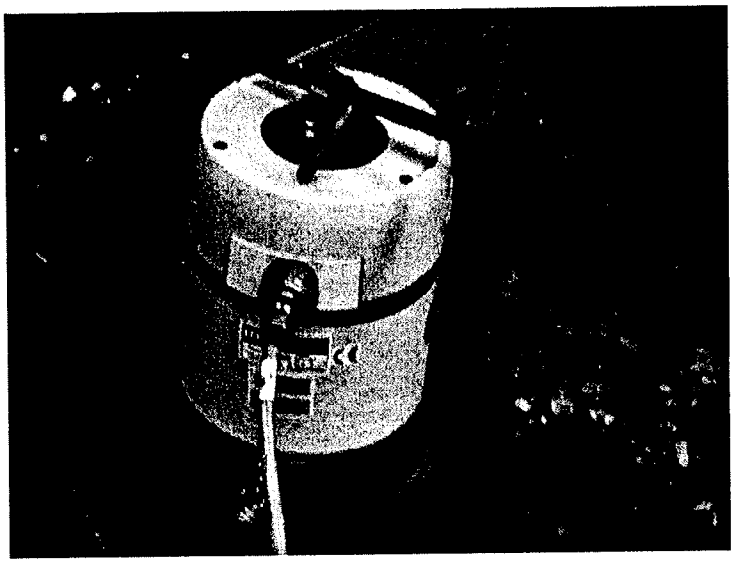

Photograph 3: Vibrator

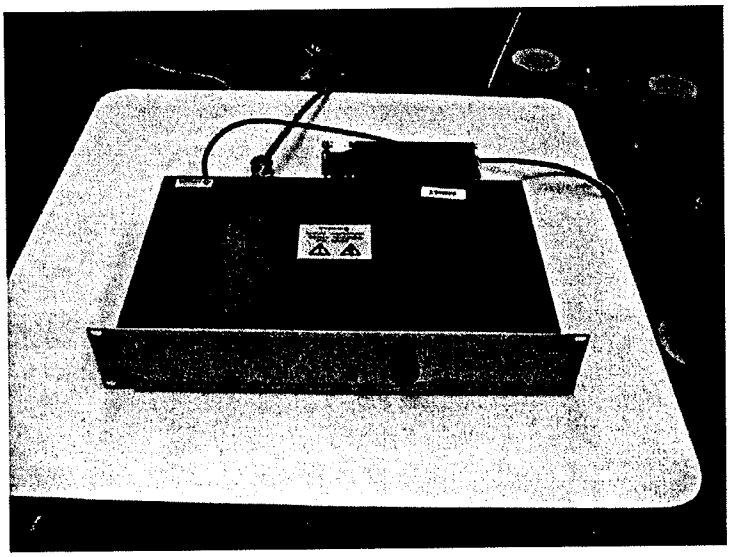

Photograph 4: Amplifier for Vibrator

Photograph 5:
Accelerometer

Photograph 6:
Signal Conditioner

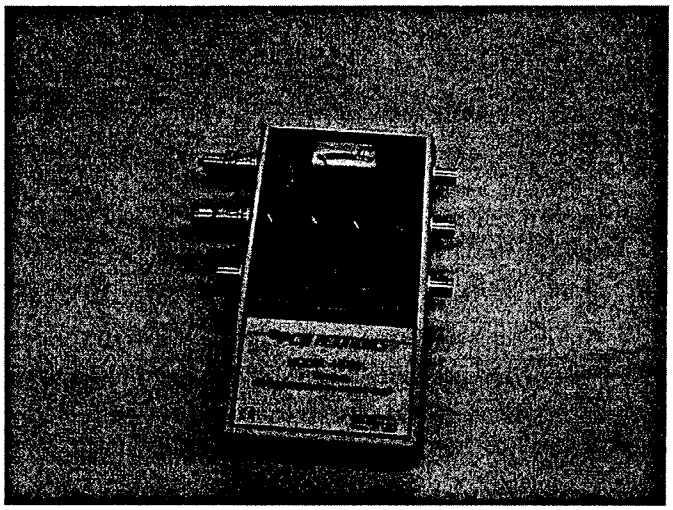

Photograph 7:
Data Acquisition

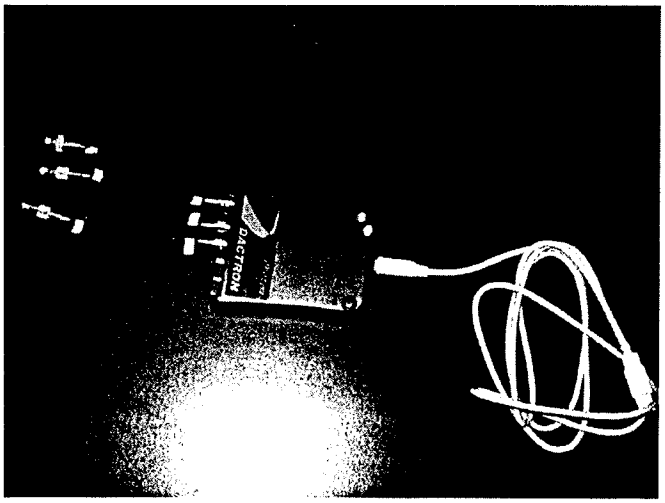

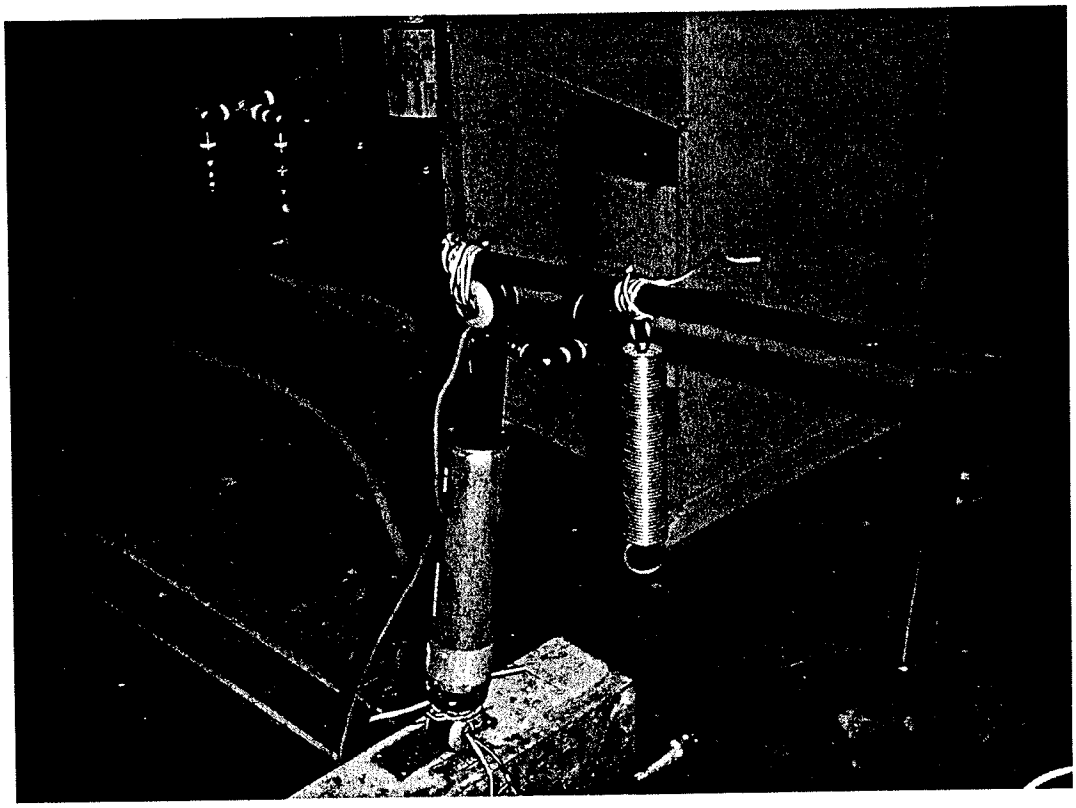

Photograph 8 MR Damper Connected with Cable and Ground

Experimental Results

Frequency Characteristics of Stay Cable

Before installing the damper, a mass weighted 93.4N was hung at the middle point 'D' to give the cable a free vibration by cutting the chord connecting the mass. The acceleration time histories at points 'B' and 'D' were measured by two accelerometers and collected by a Photon® data acquisition system. Fast Fourier Transformation (FFT) of those time history data was carried out to form the frequency spectra. From the frequency spectra, the basic natural frequency of the cable without damper was obtained as 8.93Hz with a cable axial tension force of 16.06KN. Since the scaling factor used is eight (8), the frequency of the prototype should correspondingly be 1.12Hz, which is within the reasonable range of the actual cable frequency (Tabatabai et al. 1998). Theoretically, the cable natural frequency can be calculated by the following equations (Irvine 1981):

$$\tan(\Omega/2) = \Omega/2 - (4.0/\lambda^2)(\Omega/2)^3 \qquad (1)$$

$$\Omega = 2\pi fL/\sqrt{T/m} \tag{2}$$

$$\lambda^2 = (\frac{mgL\cos(\alpha)}{T})^2 L \Big/ \frac{TL_e}{EA} \tag{3}$$

$$L_e = (1 + \frac{(\frac{mgL\cos(\alpha)}{T})^2}{8})L \tag{4}$$

in which, E is the Young's modulus, T is the tension force, L is the cable length, α is the inclined angle, L_e is the deformed cable length (Assumed as a parabolic deflected shape), A is the cross section area, m is the mass per unit length, and λ^2 is proportional to the ratio of the axial stiffness to the geometric stiffness. It is a non-dimensional parameter to describe the cable dynamic behavior.

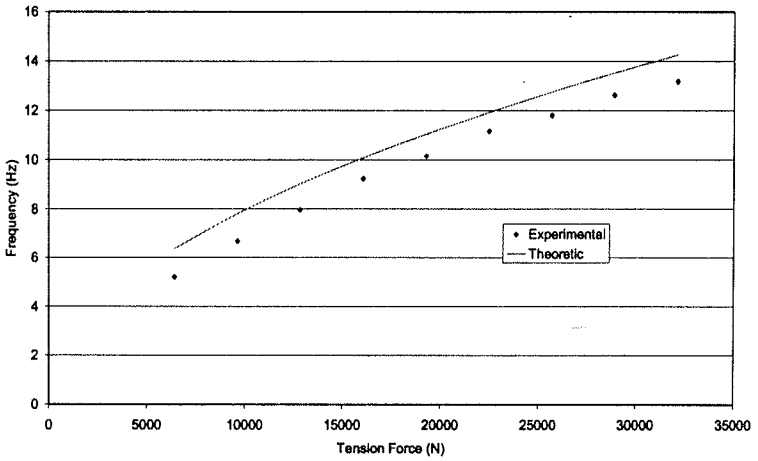

Fig. 9: The Cable Natural Frequencies

From Eqs. (1)~(4), the frequency f can be calculated as 10.08Hz, which is 12.9% higher than the experimental result. If the tension force is changed, the natural frequency of the cable will also change. The theoretical and experimental frequencies versus tension forces are plotted in Fig. 9.

Free Vibration

After testing the pure cable, the MR damper was then connected to point 'B' to reduce the cable vibration. The acceleration time history of point 'D' is plotted in Fig. 10, in which all the data are normalized for the convenience of comparison. It can be observed from Fig. 10(a) that even if there is no current provided, the damper provides very large damping so that it reduces the cable vibration efficiently. Fig. 10(b) shows when the current reaches 0.1A, the acceleration response is reduced more quickly than the 0A case. Fig. 10(c) shows the acceleration time history data with currents of 0.1A and 0.2A from 0 to 1.5 seconds. It can be observed that the damper with 0.2A current reduces

the vibration slightly more efficient than that of 0.1A case at the beginning when vibration is large and is almost the same after 0.5 second when the vibration is small. This is because, on one hand, when the measured signals are small, the relative error due to the noise is larger. On the other hand, since the MR damper can be considered as a Bingham element, it needs a larger force (or vibration) to overcome the Coulomb friction to pull and push the damper when the current becomes larger. If the driving force provided by the cable vibration is not enough, the MR damper will work as a fixed support (or locked). In that case, the damping effect under different currents beyond a critical current will not differ much.

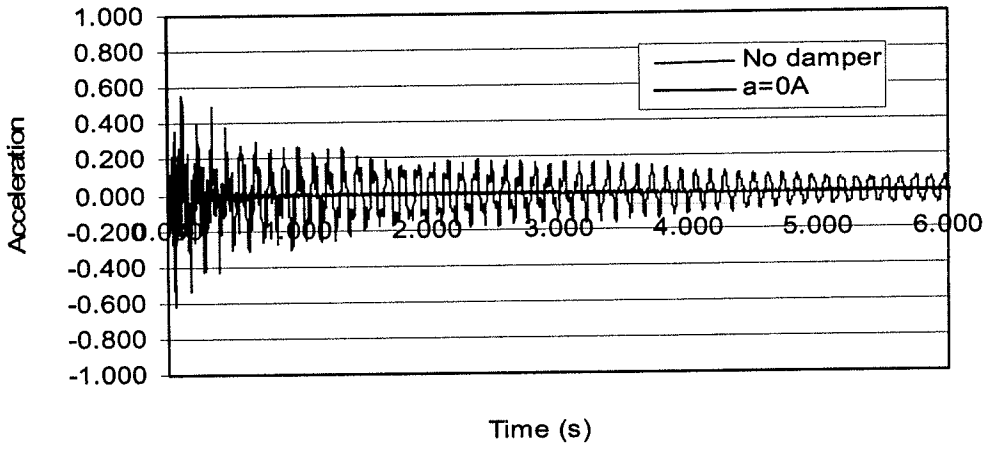

(a) Efficiency of 0A Current

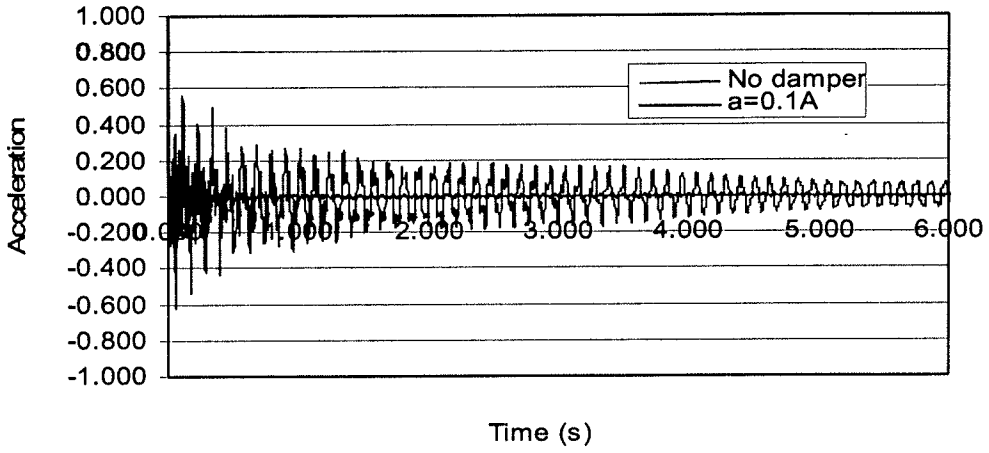

(b) Efficiency of 0.1 Current

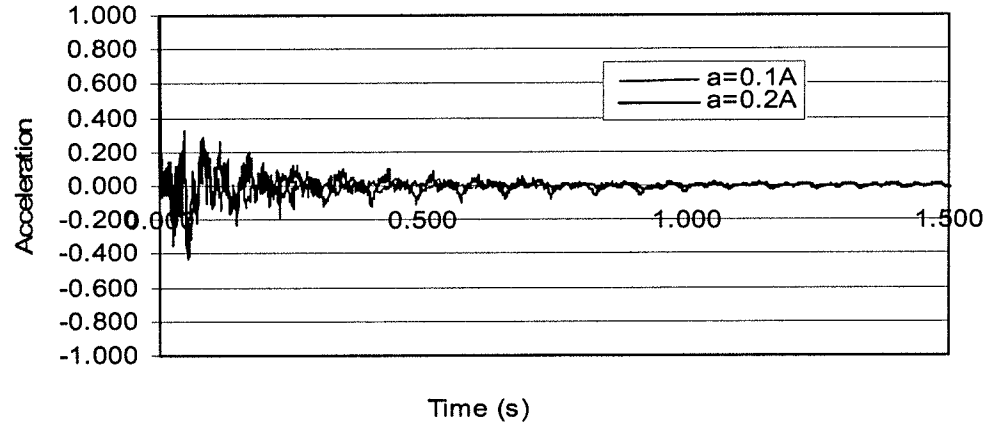

(C) Comparison: 0.1A and 0.2A

Fig. 10: Acceleration Response of Cable with MR Damper

Forced Vibration

For the forced vibration, instead of using a hanging mass, a shaker (vibrator) working as an excitation source was put 0.18m away from the low end of the cable. It is 2.3% of the whole cable length.

Fig. 11 shows the acceleration response with a 10Hz sine wave excitation. From this figure, it is observed that the stable cable vibration with a damper of 0.1A current is much less than that without damper. The ratio of the peak value between the case of 0.1A current and no damper is about 14.

Fig. 12 shows the peak acceleration response of different cases. In Fig. 12(a), the acceleration is normalized with the peak acceleration of the case without damper for each excitation frequency. This figure shows that the effect of reduction is much better at the 9Hz excitation, which corresponds to the resonant frequency of the cable system. When the excitation frequency is away from this resonant frequency, the reduction efficiency decreases correspondingly. Fig. 12(b) shows more clearly the high reduction efficiency around the resonant frequency for each current, and the resonance frequency increases slightly with the increase of current. This means that the stiffness of the damper increases with the damper current so that the natural frequency of the cable-damper system becomes larger. This phenomenon is similar to the case when a conventional viscous damper was added to the cable end (Main and Jones 2002a, 2002b). More experimental results are given in Appendix B.

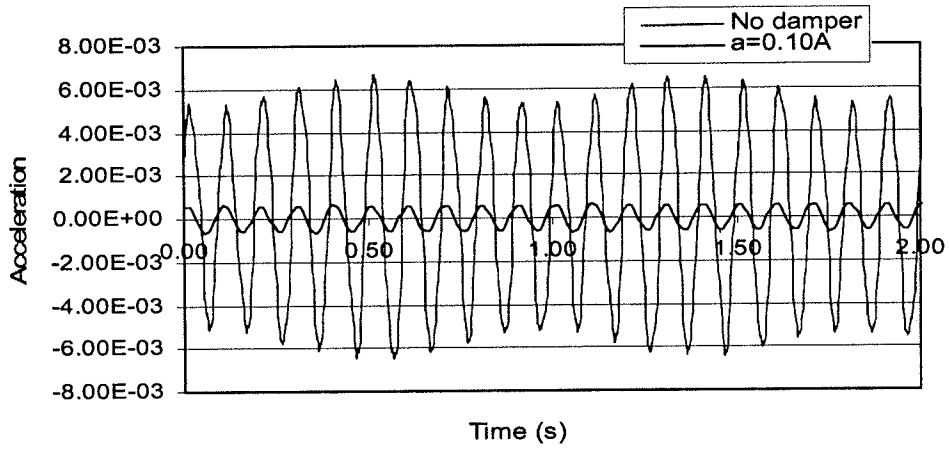

Fig. 11: Cable Acceleration Response under Forced Vibration

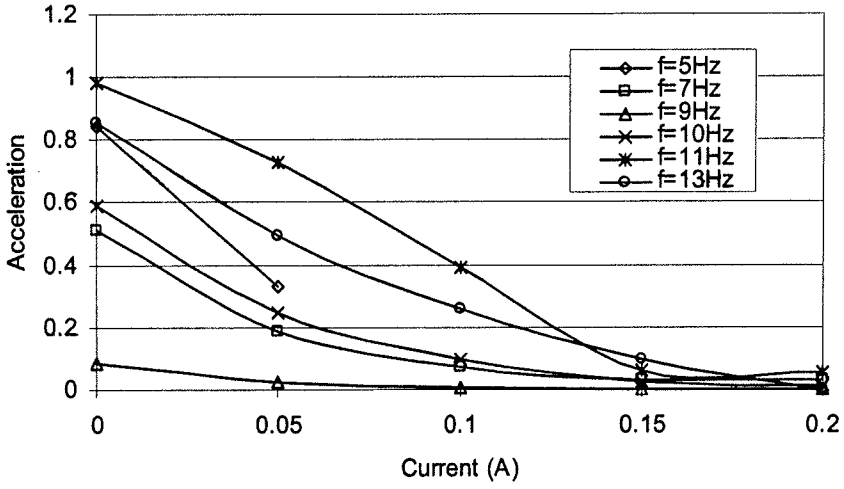

(a) Acceleration versus Current

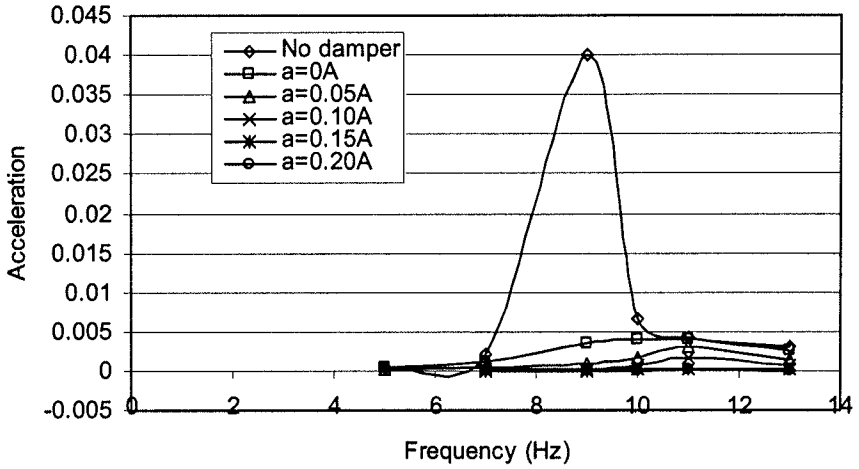

(b) Acceleration versus Frequency

Fig. 12: Peak Acceleration Response of Cable Vibration

Cable Vibration Control with TMD-MR Dampers

Concept and Principle of TMD-MR Damper

TMD dampers have been used extensively in structural vibration control. The concept of vibration control by TMD dampers can be stated as follows. The interaction between any two elastic bodies can be represented with a two-mass system shown in Fig. 13. Under the excitation of a sinusoidal force *Fsin(ωt)* acting on mass 1, the vibration amplitudes of this two-mass system are derived as

$$X_1 = \frac{Fm_2(\omega_{m_2}^2 - \omega^2)}{(k_1 + k_2 - m_1\omega^2)(k_2 - m_2\omega^2) - k_2^2},\quad X_2 = \frac{Fm_2\omega_{m_2}^2}{(k_1 + k_2 - m_1\omega^2)(k_2 - m_2\omega^2) - k_2^2} \quad (5)$$

where $\omega_{m_1}^2 = k_1/m_1$ and $\omega_{m_2}^2 = k_2/m_2$. It can be seen from Eq. (5) that when $\omega_{m_2}^2 = \omega^2$, the vibration amplitude of Mass 1 vanishes with $X_1 = 0$ and the amplitude of Mass 2 will be $X_2 = F/k_2$.

Many pairs of components on the bridge can be visualized as this two-mass system, such as cable-deck/tower pair. If the frequencies of the cable and the deck/tower are close to excitation frequency ω, the energy of bridge vibration corresponding to that particular frequency ω will be passed to the cable. This energy could be a large amount compared to the masses of cables. Therefore, the natural frequency of cables should be designed away from the significant frequencies of the bridge to avoid resonant vibrations.

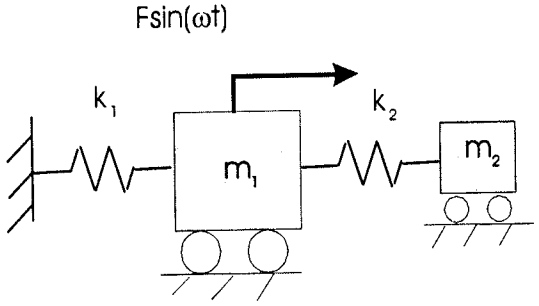

Fig. 13: A Two-mass System

The basic concept of cable vibration control by using TMD-MR damper is similar to the TMD control as shown in Fig. 14 where the cable mass and the TMD mass represent m_1 and m_2, respectively, as discussed above. The MR damper will provide an adjustable damping and stiffness. When MR dampers are not used in Fig. 14, then it is called TMD system, otherwise it is called TMD-MR system. The developed TMD-MR damper system will then be installed on the cable as shown in Fig. 15.

Since the cable vibration is a very complicated phenomenon and there is not only one natural frequency for the vibration mechanism, the supplemental damping of MR damper to the TMD-MR damper system can provide several advantages for the vibration control strategy. The first is the TMD function and is called TMD component hereafter.

When the cable natural frequency changes, the MR damper can help adjust the natural frequency of the TMD-MR damper system to trace the resonant excitation frequency so that the TMD-MR damper can be effective for a range of cable vibrations. The second is the MR damper function and is called MR component hereafter. When there are more than one dominating cable natural frequencies or when it is hard to tune the TMD frequency to a specific value, MR component can still hope to work effectively since it can provide considerable output damping force and its damping efficiency is relatively frequency insensitive as observed earlier. More importantly, the MR damper can still work as a passive damper when the control strategy fails.

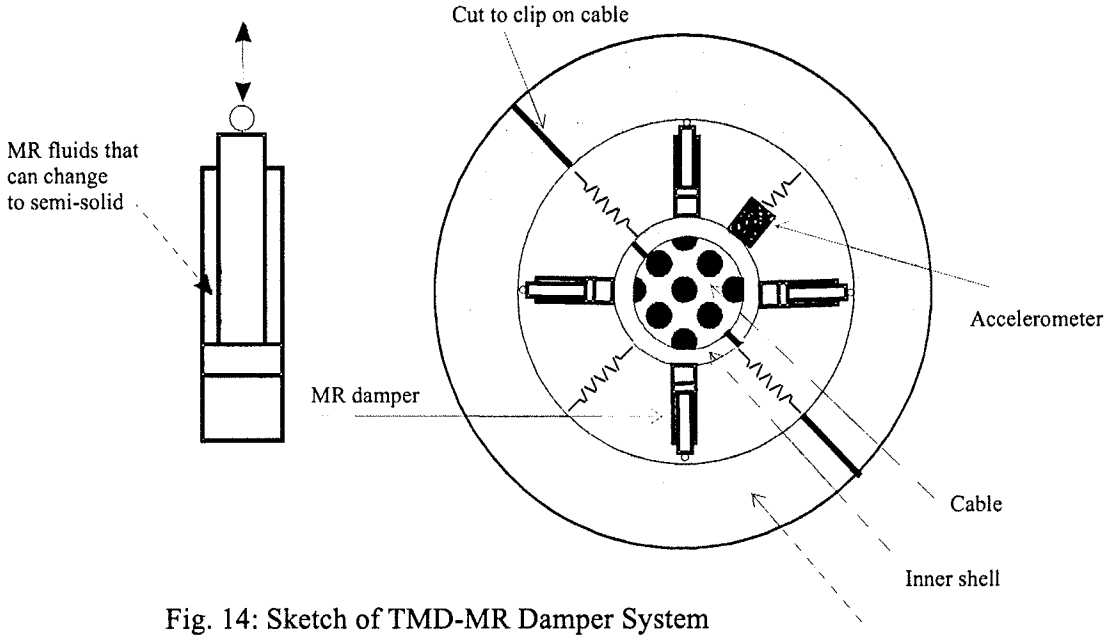

Fig. 14: Sketch of TMD-MR Damper System

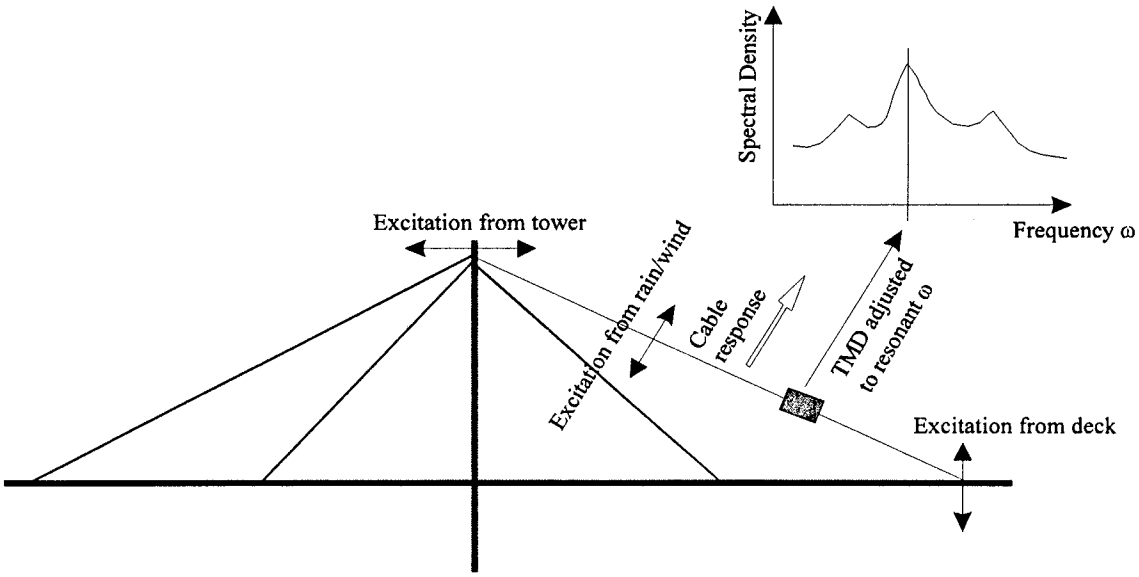

Fig. 15: Sketch of Cable Vibration Control

Adjustable TMD-MR Damper Design

None of the companies we contacted has available MR dampers with small force and size to match the model cable used in the present investigation. Therefore, we need to design and manufacture those dampers ourselves. Two pressure driven flow modes with different sizes were designed and one of them was chosen for the TMD-MR damper system, and one type of direct shear mode was designed and discarded because of the maintenance problem, such as oil leaking. Generally, MR damper design consists of two steps: geometry design and magnetic circuit design. The main design process, which follows Lord Corporation Engineering Note (1999), is summarized in the Appendix C for reference.

Based on the information of Appendix C, more design cases are compared virtually and the following two optimal designs are chosen for comparison as listed in Table 4. All the length units in Table 4 are millimeter. The definitions of r_1 to r_4 are marked in Fig. 16.

Table 4: Design Parameter for Pressure Driven Flow Damper (unit: mm)

Designed Data										
	r_1	r_2	r_3	r_4	t	g	L	d	τ_y (pa)	η ($pa \cdot s$)
Type 1	10	8	7.6	3	2	0.4	1	10	45000	4
Type 2	10	8	7.5	4	2	0.5	1.5	10	45000	8
Calculated Data										
	F_τ (N)		F_η (N)		λ					
Type 1	86.2		6.8		12.7					
Type 2	42.7		3.7		11.5					

Fig. 16 shows the sketch of the assembled shaft and sleeve. Fig. 17 and Fig. 18 show the details of the sleeve and the shaft of the first design case in Table 4.

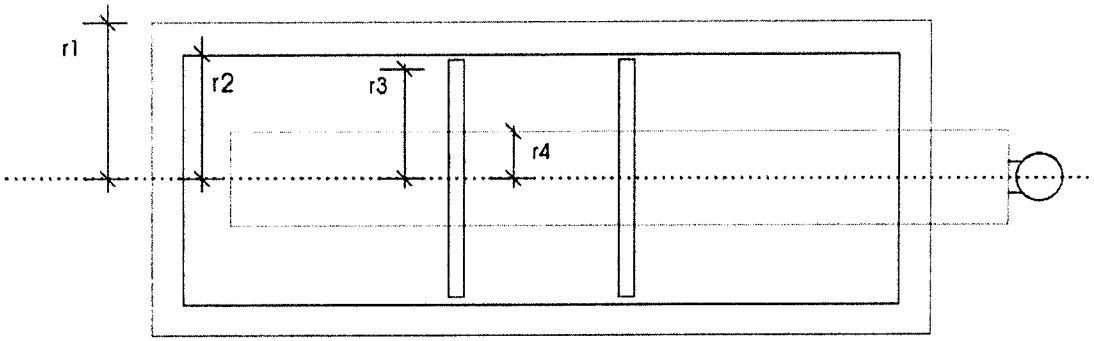

Fig. 16: Sketch for Designed MR Damper

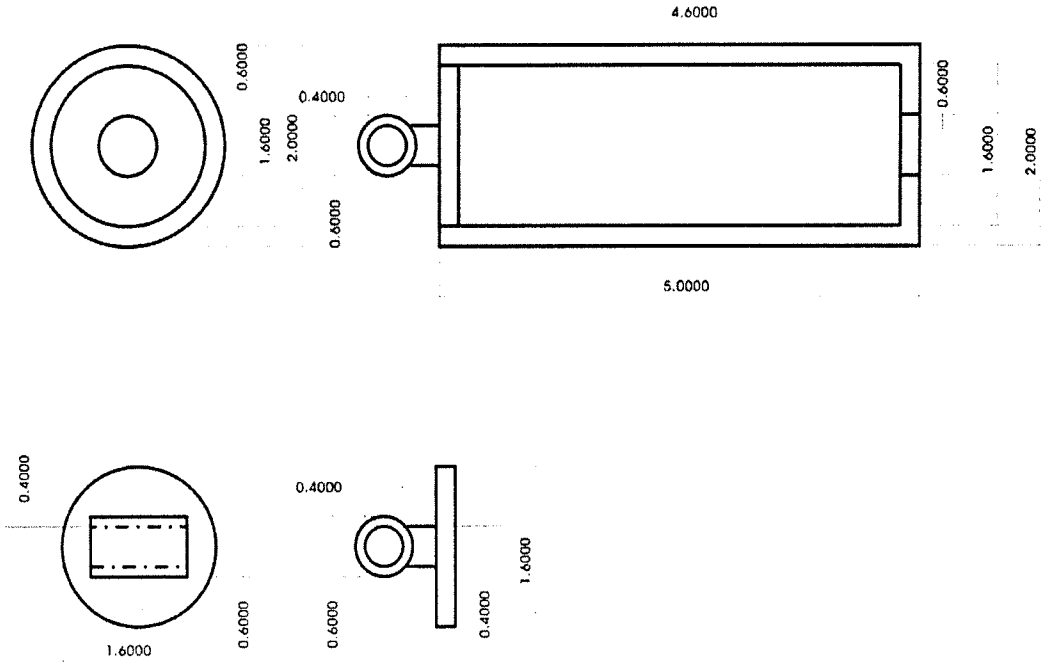

Fig. 17: Details of the Designed Sleeve

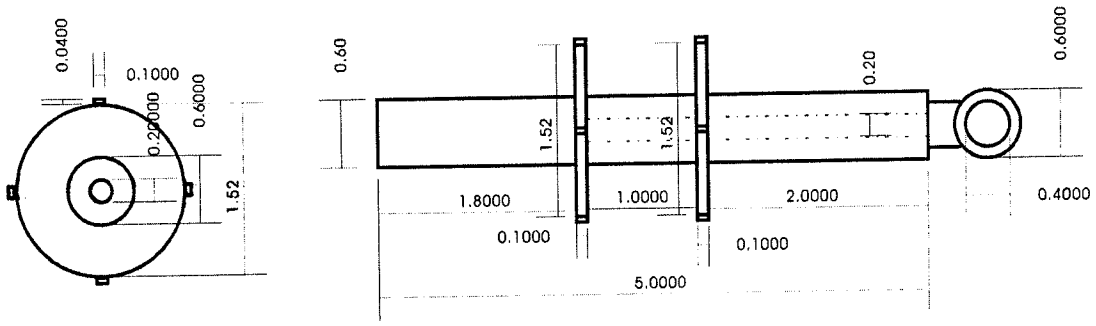

Fig. 18: Details of the Designed Shaft

Cable-TMD-MR System: Theoretical Analysis

Problem Statement

To study the cable-TMD-MR system theoretically, the effect of gravity is neglected and a horizontal cable configuration is chosen for simplicity. The problem under consideration is depicted in Fig. 19. A TMD-MR damper system is hung on the cable at an intermediate point, dividing the cable into two segments. Without losing generality, we assume $l_2 > l_1$. For the considered problem, the following assumptions are made:

1) The tension force in the cable is large compared to its self-weight, so the vertical sag is small and can be neglected.

2) The bending stiffness and internal damping of the cable is small.

3) The deflection is small so that the secondary tension force caused by cable deflection is neglected.

4) The TMD-MR damper is modeled as an equivalent system with a spring parallel with a dashpot.

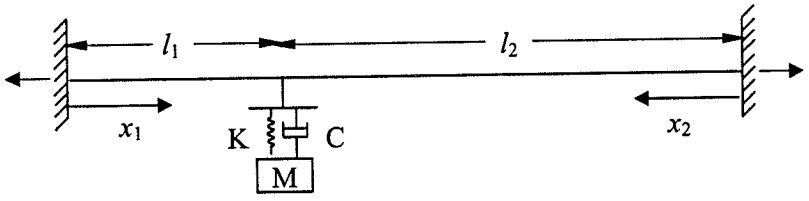

Fig. 19: Cable-TMD-MR System Model

With these given conditions, the following partial differential equation is satisfied over each segment of cable:

$$T\frac{\partial^2 v_k(x_k,t)}{\partial x_k^2} = m\frac{\partial^2 v_k(x_k,t)}{\partial t^2} \tag{6}$$

where T is the axial tension force in the cable; m is the mass per unit length; x_k is the coordinate along the cable of the k th segment and v is the transverse deflection. A nondimensional time $\tau = \omega_c t$ is introduced to simplify the expression, and $\omega_c = (\pi / L)\sqrt{T/m}$ is the fundamental natural frequency of the cable. Solution for this equation is discussed in Appendix D.

Numerical Examples

According to Appendix D, when all the other parameters are specified for a particular cable, the nondimensional complex eigenvalue s in Eq. (D-12) of Appendix D can be solved by the Newton iteration method. Then the system damping ζ that is defined in Eq. (D-13) can be obtained. This information can be used to guide the TMD-MR design as shown below.

Incidences of wind-rain induced vibrations have been widely reported to be detrimental to cables of cable-stayed bridges recently (Hikami 1986, Matsumoto et al. 1992). In the following discussions, the emphasis is placed on the wind-rain vibration issues. Irwin (1997) proposed the following criterion to control the wind-rain induced cable vibration,

$$S_c = \frac{m\zeta}{\mathrm{P}D^2} \geq \alpha \tag{7}$$

where S_c is the Scruton number; P is the mass density of air; D is the outside diameter of cable; and α is the limiting value for Scruton number. The relationship in Eq. (7) can be rewritten as

$$\zeta \geq \frac{\alpha \mathrm{P}D^2}{m} = \frac{\alpha}{\mu} \tag{8}$$

where the mass parameter μ is defined as $\mu = m/PD^2$. Therefore, to meet the above stated criterion, the damping ratio of the cable needs to meet the requirement of Eq. (8). Based on available test results, Irwin (1997) proposed a minimum α of 10.

The modal damping of a stay-cable is composed of the intrinsic damping and the additional damping provided by damping devices. The former is typically low and cannot be reliably estimated. In this calculation, the intrinsic damping of the cable is conservatively ignored. The following example is used for demonstrating a preliminary design process.

This example was also used by Tabatabai and Mehrabi (2000). Assume that a cable with the properties listed in Table 5 is in need of a TMD-MR damper to suppress wind-rain induced vibrations. To design a TMD-MR damper with its frequency tuned to the first mode, the following process can be followed.

Table 5: Properties of example cable

m ($kg \cdot m^{-1}$)	L (m)	T (N)	P (kg/m^3)	D (m)	ω_{c1} (sec^{-1})
114.09	93	$5.017*10^6$	1.29	0.225	7.08

1) Determine the demanding modal damping ratio

Since the mass parameter μ can be calculated as $\mu = m/PD^2 = 1747$, the demanding modal damping is determined from Eq. (8) as,

$$\zeta_1 \geq \beta/\mu = 10/1747 = 0.0057 = 0.57\% \tag{9}$$

2) Determine the TMD-MR parameters

Since the TMD-MR damper is tuned to the first mode, it is placed at the mid-span to achieve the best control effect. Then, following the common practice, the mass ratio of the TMD-MR damper is chosen as 2%, from which the mass of the damper is determined as

$$M = 2\% * L * m = 0.02 * 93 * 114.09 = 212.2kg \tag{10}$$

The frequency ratio between the cable frequency and damper frequency is then chosen approximately as $\rho = 1.0$ since it is a fundamental mode tuning, from which the stiffness of the TMD-MR damper can be determined as

$$K = M(\frac{\pi}{L}\sqrt{\frac{T}{m}})^2 = 212.2*(\frac{3.14159}{93}\sqrt{\frac{3.017*10^6}{114.09}})^2 = 6403.3N/m \tag{11}$$

By solving the cable equations in Appendix D, the relationship between the damper damping ratio ξ and system modal damping ratio ζ, i.e., the design aid curve, can be developed as shown in Fig. 20(a) for the first mode tuning. Shown in the figure are also the curves for a few modes with odd numbers since the damper placed at the mid-span has no effect on the vibration of modes with even numbers (these mode shapes have zero values at the mid-span point). This figure is then referred to determine the equivalent damping ratio for the MR damper. If an actual first system modal damping $\zeta_1 = 1\%$ is chosen so that a safety factor of $1\%/0.57\% = 1.75$ can be achieved, the equivalent

damping ratio ξ is thus obtained from Fig. 20(a) as 2.6% by interpolation method. Once the required equivalent damping ratio ξ of the MR damper is known, a preliminary design for the MR damper (such as its MR liquid and current) can be performed (Li et al 2000), which is out of the scope of this work.

For the same cable, if the damper is located at the 1/4th point of the cable length to target the second mode vibration control, the stiffness of the damper is determined as,

$$K = 4M(\frac{\pi}{L}\sqrt{\frac{T}{m}})^2 = 4*212.2*(\frac{3.14159}{93}\sqrt{\frac{3.017*10^6}{114.09}})^2 = 25613.2N/m \qquad (12)$$

Then, similarly, Fig. 20(b) is referred to determine the equivalent damping for the MR damper. It is noted that the damper located at the 1/4th point of the cable length has no effect on the vibration of the fourth mode (this mode shape has zero value at the 1/4th point of the cable length). An actual modal damping $\zeta_2 = 1\%$ is also chosen so that equivalent damping ratio ξ is obtained from Fig. 20(b) as 2.54%.

In addition to the wind-rain induced cable vibration, other types of cable vibrations such as those due to vortex excitation, galloping, etc. are also concerned. However, if a target cable damping ratio is defined for those specific types of vibrations, the design process proposed here is also applicable. For a refined optimal design, much more calculation is necessary to construct design curves that relate the damping ratio of the TMD-MR to the system modal damping of the cable-damper system under different parameters. Simultaneous multimode cable vibration control and adaptive control also deserve further studies, which will be pursued by the writers once the basic behavior of the cable-TMD-MR system is fully understood.

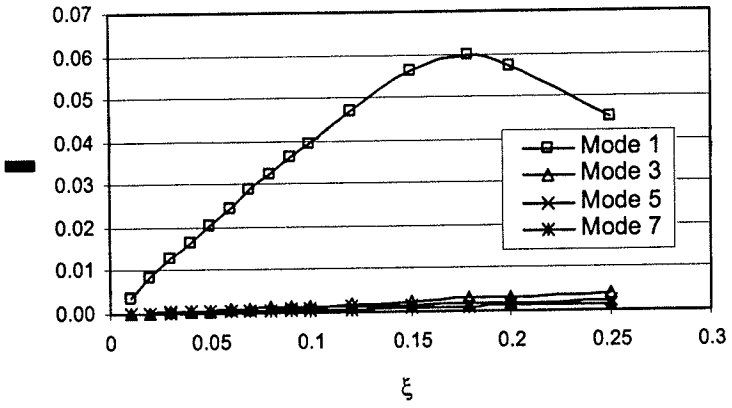

(a) Design curve of 2% mass ratio, first mode tuning

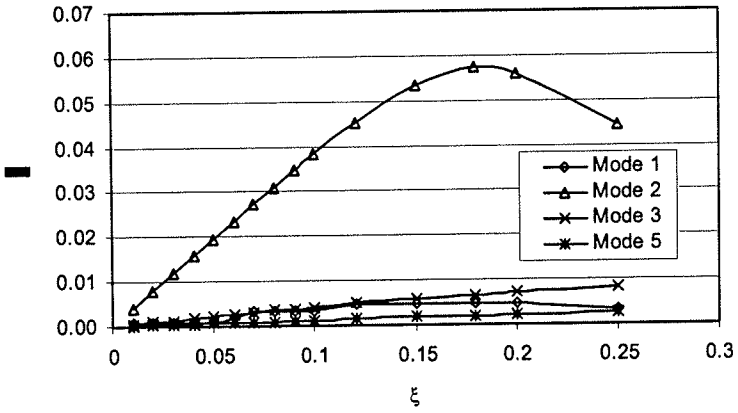

(b) Design curve of 2% mass ratio, second mode tuning

Fig. 20: System Modal Damping Ratio vs. Damper Damping Ratio

Cable-TMD-MR System: Experiments

General Discussion

After the TMD-MR damper was designed, it was installed on the cable with a tension force of 16.06 kN. The parameters of the cable-TMD-MR damper system are listed in Table 6. Since adding MR damper would affect the natural frequency of the TMD-MR damper system, the frequency of TMD damper was designed as about 7Hz, which is less than the cable natural frequency 8.93Hz, obtained from previous experiments for a tension force of 16.06 kN. One accelerometer was put on the cable and the other one on the outside circle of the TMD-MR damper so that the acceleration of both the cable and the TMD-MR damper can be measured as shown in Photograph 9. Since just the relative value of the cable acceleration with or without the TMD-MR damper was concerned, the unit of the measured acceleration is chosen as the unit of electronic signal volts. However, it is easy to change the electronic unit to the kinematics unit since 9.84mV equals to 1.0g according to the sensor specifications. Two baffles were installed on the cable to prevent the out of plane vibration of the TMD-MR damper.

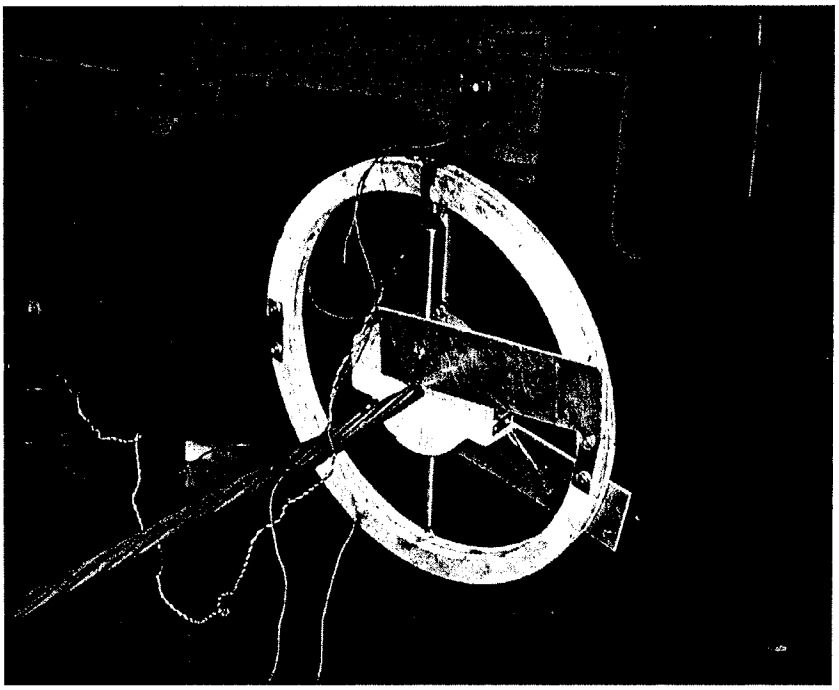

Photograph 9: TMD-MR Damper on the Cable

The following figures are results with a tension force of 16.06kN. Fig. 21 shows the acceleration time history of the cable. It is observed that when there is no damper attached on the cable, the vibration is the largest. When the TMD or TMD-MR damper is attached on the cable, the cable vibration is reduced to different extents. From Fig. 22 and Table 7, we can find that the TMD-MR damper can reduce the cable vibration down to

about 20% from the power spectral density (PSD) perspective. It is verified again that there is some saturation effect, as the reduction effects are pretty close for the 0.15A and 0.2A cases. We can observe from Fig. 23 that with the increase of current inside the MR damper, the vibration decreases for both the cable and the TMD-MR damper. This means that the existence of the MR damper also helps reduce the TMD vibration. The reduction effect of pure TMD is between that of the TMD-MR damper with 0A current and 0.05A current. From Fig. 23(b), we can also observe that the TMD damper vibrates the largest in the case of cable with TMD only, which means that the cable vibration has been transferred to the TMD vibration.

Table 6: Parameters of Cable-TMD-MR Damper Experiments

TMD-MR Damper	Mass	Upper Spring Stiffness	Lower Spring Stiffness
	0.3175 Kg	304.5 N/m	481.25 N/m
Cable-TMD-MR System	TMD-MR Location	Frequency Ratio	Mass Ratio
	Middle of the cable or point "D" in Fig. 8	1.27	0.06
Parameters Variation Range	Tension (kN)	Current in MR damper	Control Experiments
	12.85-32.13	0~0.20A	No damper, TMD only

Table 7: Cable Vibration Reduction by TMD and TMD-MR Damper (Ratios of Controlled over uncontrolled vibration)

Case	TMD only	0A	0.05A	0.10A	0.15A	0.20A
Effect	27.1%	28.2%	21.3%	20.8%	20.2%	19.7%

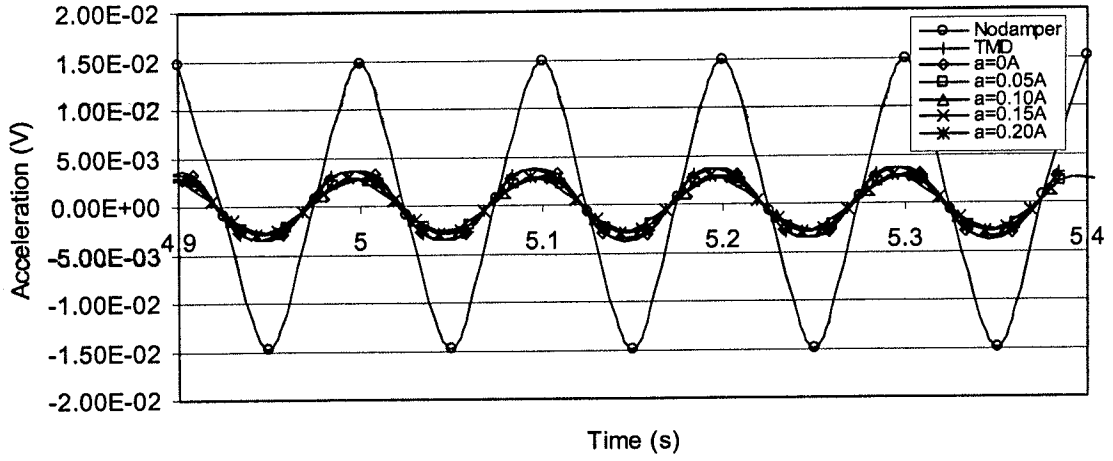

Fig. 21: Acceleration of Cable

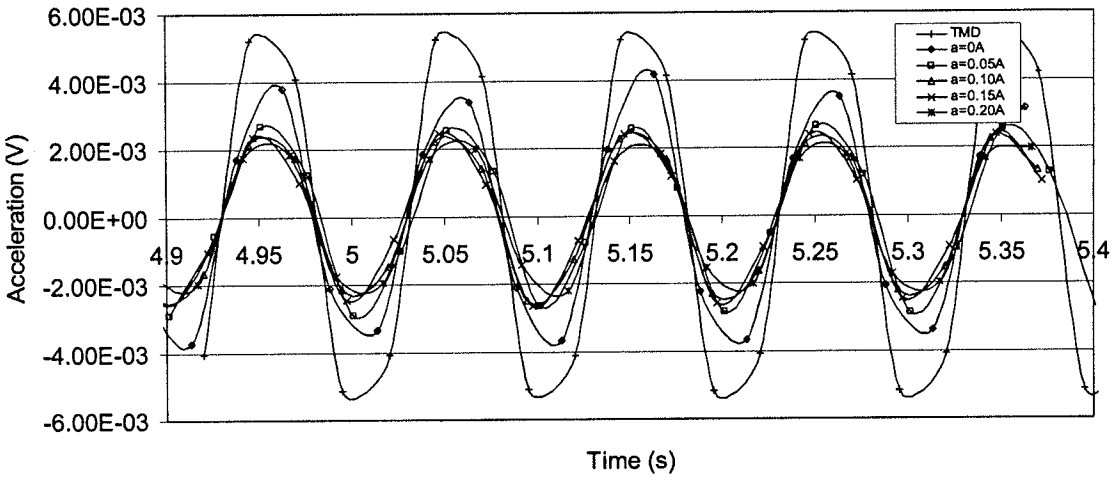

Fig. 22: Acceleration of TMD-MR Damper

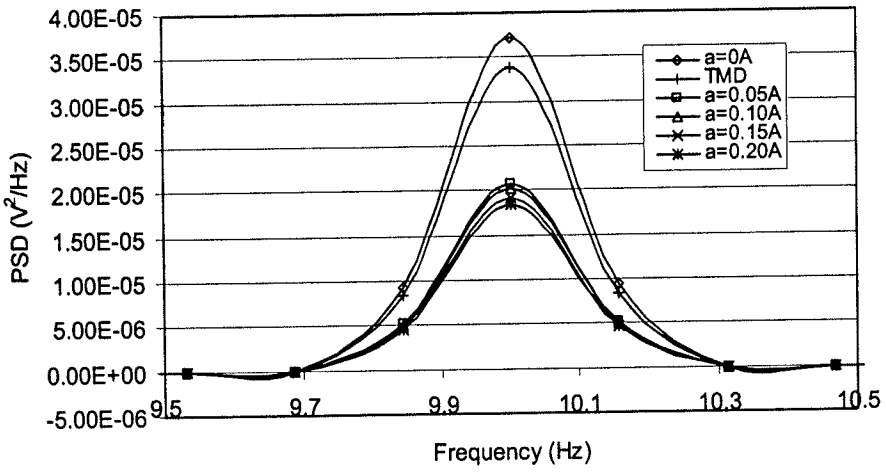

(a) Cable

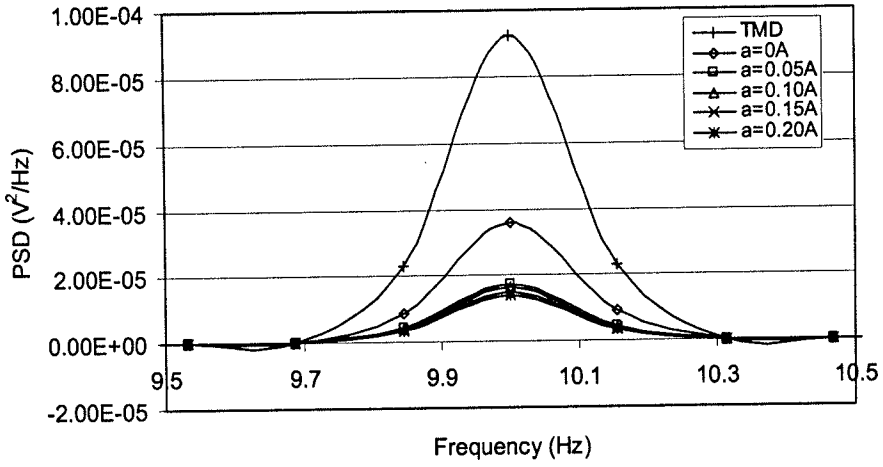

(b) TMD-MR Damper

Fig. 23: Power Spectral Density (a) Cable, (b) TMD-MR

Vibration Energy Transfer

From the perspective of energy, the goal of structural control is using control device to absorb and dissipate the structural vibration energy. In the following figure that is based on TMD only (without MR damper), we are going to discuss more about the vibration energy transfer with free vibration results.

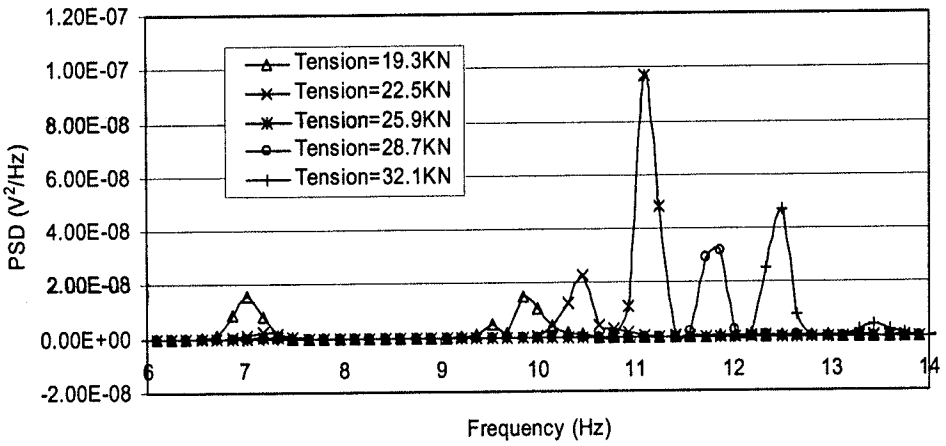

(a) Cable

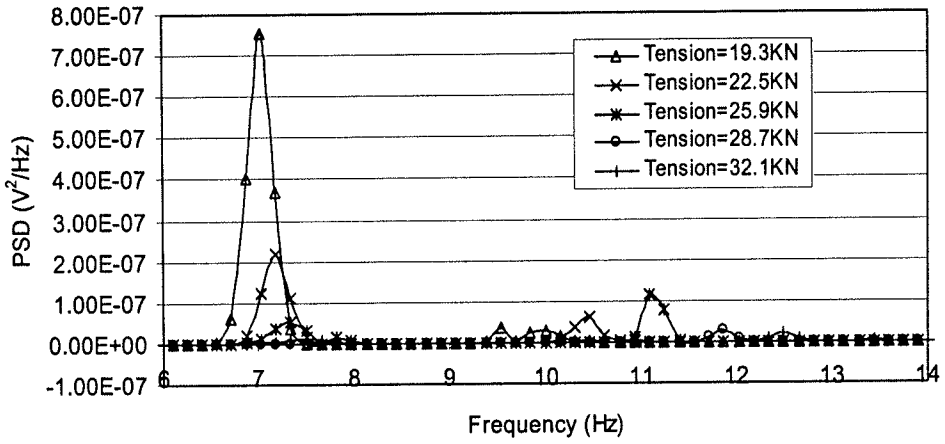

(b) TMD Damper

Fig. 24: Power Spectral Density of Cable-TMD System with Different Tension Force (a) Cable, (b) TMD

From Fig. 24, it can be observed that there are two PSD peaks for each cable tension force. One peak is related to the natural frequency of the TMD damper and the other is related to the natural frequency of the cable. With the increase of the tension force, the natural frequencies of both the cable and the TMD damper increase. This means that the measured cable frequency and TMD damper frequency are not pure cable frequency and pure TMD damper frequency any more. The frequency of cable has included the influence of the TMD damper and vice verse. As shown in Fig. 24(a), take cable force of 25.9 kN for example, the vibration energy mostly centralizes around the natural frequency of the cable (around 11.09 Hz) and the energy corresponding to the TMD damper natural frequency is pretty small (around 7.0Hz). However, in Fig. 24(b), the vibration energy around the natural frequency of the TMD damper (around 7.0Hz)

dominates and the energy corresponding to the cable natural frequency (around 11.09 Hz) is significantly less, which means that the energy has transferred from the cable to the TMD damper.

Frequency Shift

Adding dampers to the cable will always affect the cable natural frequency. Main and Jones (2002) discussed the shift of cable frequency due to the supplemental viscous dampers. According to the experimental results, adding TMD-MR or TMD will also affect the natural frequency of the cable. From Table 8, we can see that by adding the TMD damper, the frequency of the cable-TMD system is less than that of the pure cable, though the frequency shift is small.

Table 8: Frequency Shift of Cable-TMD System

Tension (kN)	19.3	22.5	25.9	28.7	32.1
Frequency of pure cable (Hz)	10.16	10.94	11.72	12.5	13.13
Frequency of cable-TMD (Hz)	9.84	10.47	11.09	11.88	12.5

Factors Affecting Vibration Reduction Effect

As stated earlier, adding TMD-MR damper not only improves the cable damping, but also changes the natural frequency of the cable system. The mass of the TMD-MR damper used in this experimental study is about 6% of the entire cable weight. Fig. 25 plots the maximum acceleration of different cable experimental setups. Table 9 defines the case number that is shown as the X-axis in Fig. 25 and the corresponding experimental setup.

Table 9: Experiment Setup in Figure 25

Case Number	1	2	3	4	5	6	7
Experiment Cases	No damper	TMD only	Passive (a= 0A)	A=0.05A*	a=0.10A	a=0.15A	a=0.20A

* Meaning that the TMD-MR damper is attached to cable with a current of 0.05A.

The following observations can be made from Fig. 25 according to the different ranges of excitation frequencies. It is noted that after the installation of the MR damper, the TMD-MR natural frequency is different from that of TMD only (7 Hz). When the excitation frequency equals to 5 Hz and 6 Hz, which is away from the natural frequency of both the cable (about 9 Hz) and the TMD-MR damper (about 8 Hz), the best vibration reduction occurs in the case of the passive TMD-MR damper (with 0A current, Case 3) for both the cable and the TMD-MR vibration. With the current inside the MR damper increases, the cable vibration increases from 0A case to 0.05A case and keeps almost the

same when the current changes from 0.05A to 0.20A. This observation verifies that larger current in the MR damper does not guarantee better vibration control effect for the cable. This phenomenon is due to several reasons. First, when the excitation frequency is away from the cable frequency and the TMD-MR damper frequency, the cable vibration is small so that the control effect of TMD-MR damper is also small. Second, a larger current in the MR damper will increase the natural frequency of the TMD-MR damper so that the stiffness change effect of the TMD-MR damper, which enlarges the cable vibration in these cases, is larger than the reduction effect due to its increase in damping.

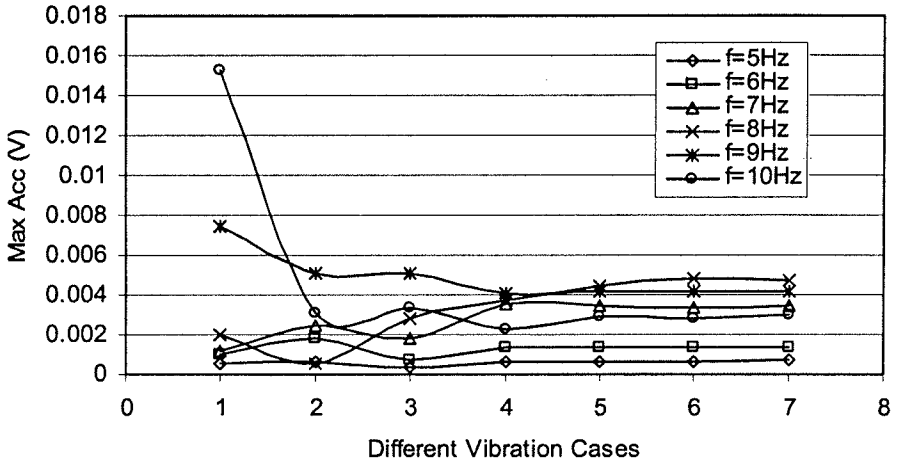

(a) Cable

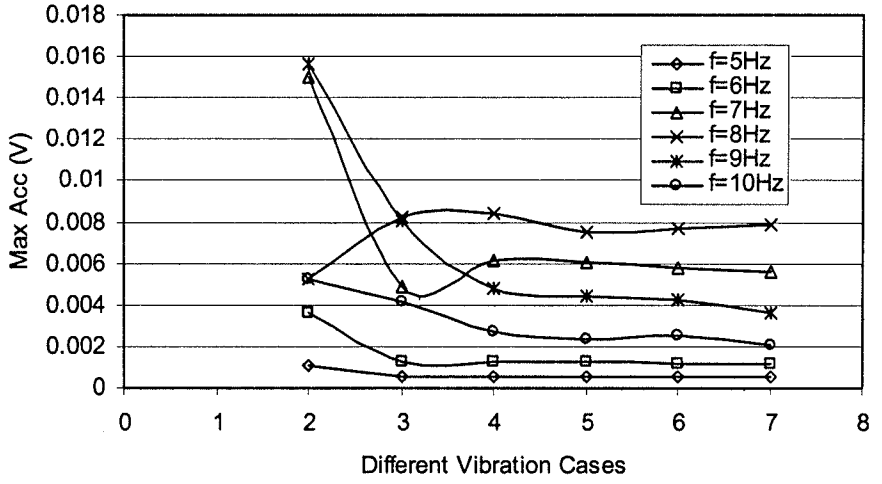

(b) TMD-MR Damper

Fig. 25: Maximum Acceleration of Cable-TMD-MR System under Different Experiment Setup (a) Cable, (b) TMD-MR

When the excitation frequency reaches 7 Hz that is close to the TMD frequency, a significant vibration is observed in the damper. When the excitation frequency reaches 8 Hz, the most noticeable reduction of vibration is the TMD only case (Case 2). In this case, the cable vibration is reduced to 17% of that of the passive cable-TMD-MR case (Case 3). The TMD damper vibration in Case 2 is also less than that of Case 3. This is because the TMD natural frequency is very close to the excitation frequency and the TMD damper achieves its optimal vibration reduction effect. With this excitation frequency, the cable vibration increases slightly with the increase of the MR damper current until the current reaches 0.15A. The TMD-MR damper vibration reduces from 0A to 0.10A and increases a little from 0.10A to 0.20A.

In all the above cases, the excitation frequency is away from the cable natural frequency so that the cable vibration is not very large even if there is no supplemental damper. When the excitation frequency reaches 9 Hz or 10 Hz, the pure cable vibration is about 1 or 2-order larger than that with excitation frequency away from the cable natural frequency. The effect of the TMD-MR damper becomes obvious in these resonant vibration cases. The vibration of the cable for the passive TMD-MR damper case (Case 3) is close to that of TMD only case (Case 2) and much smaller than that of pure cable case without dampers (Case 1). Increase of the current from 0A to 0.05A leads to a smaller cable vibration, from 0.05A to 0.10A leads to a little larger cable vibration and from 0.10A to 0.20A leads to an almost constant cable vibration. Comparing these 9 Hz and 10 Hz cases with those of 5 Hz and 6 Hz, it is observed that the current in the MR damper corresponding to the best reduction effect increase from 0A to 0.05A and the current corresponding to the beginning of saturation increases from 0.05A to 0.10A. This observation shows that TMD-MR damper is more suitable for reducing large cable vibration.

Some observations made above are summarized below.

1) Effect of excitation frequency

The relationships among the natural frequencies of the cable, the TMD-MR damper, and the excitation forces will affect the cable response significantly. When the excitation frequency is away from that of the cable and the TMD-MR damper, the cable vibration is not large, and the TMD-MR damper will reduce the cable vibration mainly depending on the MR component with two effects – providing additional damping and stiffness. When the MR component is in its passive mode, it provides damping and very small additional stiffness. However, when the current in the MR component increases, the stiffness and so the natural frequency of the TMD-MR damper changes, and so does the cable natural frequency. This change may cause the cable to vibrate more since the stiffness change effect may be larger than the increased damping effect. That may help to explain the observation that the cable vibration reduction effect gets worse with an increased current in Fig. 25. Therefore, when the vibration is small, the TMD-MR damper should be set to its passive mode.

When the excitation frequency is close to the TMD-MR damper while still away from the cable frequency, the cable vibration will be damped out mainly due to the TMD component. However, the vibration of the TMD-MR damper may still hard to tell because of the following reasons. On one hand, the vibration of TMD-MR should be large because it absorbs the cable vibration energy, while on the other hand, the vibration of TMD-MR damper would be small because the MR damper can dissipate energy. The actual vibration of the TMD-MR damper depends on the balance of these two effects. When the excitation frequency is close to cable natural frequency, both the TMD component and the MR component of the TMD-MR damper system can work efficiently so that the vibrations of both the cable and the TMD-MR are reduced.

2) TMD component versus MR component of TMD-MR system

The observation of test results suggests that the TMD-MR natural frequency should be tuned to the natural frequency of the cable. As a result, when the excitation frequency is away from the cable natural frequency, the cable itself will not vibrate much and MR component with small current will be enough to reduce the vibration. When the excitation frequency is close to the cable natural frequency, which is also the same as the TMD-MR natural frequency, the TMD component of the TMD-MR damper will reduce the cable vibration while the vibration will be transferred to the TMD-MR damper, which should be dissipated by MR component with a relatively large current. This is the ideal situation. However, in the practical situation, the TMD component cannot be tuned exactly the same as the natural frequency of the cable because the cable natural frequency may change due to various reasons such as deterioration. Also, when the excitation has a wide frequency range and the TMD component cannot be efficient for such a wide frequency range, the MR component should take more responsibility and help tune the TMD-MR natural frequency.

The plot of RMS (Root Mean Square) of the acceleration time history leads to the same observation as that of the maximum acceleration in Fig. 25. The plots of RMS are given in Appendix E.

Future Work and Implementation

The writers believe that the proposed TMD-MR damper system should be developed further to a practical product after the experimental verification and more work needs to be done to achieve this goal. This includes a detailed design and manufacturing of a prototype TMD-MR damper, application and evaluation of the proposed damper in the field, as well as corroboration of the research results.

TMD-MR Damper Design and Fabrication Consideration

As stated earlier, the TMD-MR damper has two important components to collaborate each other. The required spring constant should be relatively small and fatigue concern should be taken into account since the cable vibration is a frequent phenomenon. The TMD-MR damper needs to have a good balance of those parameters discussed in Appendix C. Leaking problem, which was experienced when the investigation group manufactured the MR damper, should not be a problem for a professional manufacturer. Thus, it is more appropriate to cooperate with Lord Corporation or other manufacturers of MR dampers, to reduce the manufacturing cost.

Field Verification

It is proposed that further research work should be carried out to verify the effectiveness of the TMD-MR damper system in controlling one or more cable vibrations in the field. Several cable-stayed bridges have been monitored, measured and evaluated recently with different retrofit methods in Alabama and Texas. There may be a good chance to verify the effectiveness of the TMD-MR damper system.

Dissemination of Research Findings

A large impediment to adopting new techniques is that practicing engineers are not readily exposed to the information. It is thus important to disseminate the research results. A presentation was made in the 17th ASCE Engineering Mechanics Conference at University of Delaware, June 2004. A poster was shown in the Economic Development Assistantship demonstration hosted by Louisiana State University and the Department of Economic Development of Louisiana. Two more abstracts have been submitted to conferences and three journal papers directly or indirectly related to the present research are under review. A website at http://www.cee.lsu.edu/~cai/wwj.htm is under construction to introduce the research.

Summary and Conclusion

The concept of developing an adjustable TMD-MR damper system has been investigated to help reduce the cable vibration and the vibration reduction efficiency has been discussed theoretically and verified experimentally. From the investigation of individual MR dampers, cable dynamics with and without TMD-MR damper, several suggestions and conclusions can be obtained as follows:

- Based on the experimental study on individual dampers, working conditions affect the output damping force of MR dampers to different extents. With an increase of currents, meaning an increase of the magnetic field, the output damping force increases accordingly. The maximum output damping force is almost a piecewise linear function of the provided current. Loading frequency does not affect significantly the output damping force, especially when the current is relatively high. Different loading waves (excitations) affect the output damping force, and the shape of the displacement-force curves. Therefore, attention must be paid when the displacement-force curve is used, for example, in a time history analysis. Temperatures affect the output damping force in a modest way.

- Based on the analytical and experimental study on the pure cables without dampers, the frequencies obtained from the theoretical calculation are reasonably close to the corresponding values obtained from experimental measurements.

- Based on experimental investigations of a cable with a MR damper, MR dampers can reduce the cable vibration effectively, regardless of free vibration or forced vibration. A MR damper can provide considerable damping even when it is in its passive mode. Generally speaking, the reduction effect of MR dampers increases with the increase of the current especially in the resonant and forced vibrations, but some saturation effect was observed. The damper is most effective for the resonant vibration cases. When the external loading frequency is away from the resonant frequency or when the vibration is small, the reduction becomes less effective. With the installation of the MR damper, the frequency of the cable-MR system becomes larger than that of the pure cable.

- Many factors can affect the performance of the MR damper in the design process. Some factors even contradict each other. Balance among all the factors should be made to design an appropriate MR damper.

- Theoretically, the effect of the TMD-MR damper on the cable-TMD-MR system damping is affected by the damper location, TMD-MR damping, and frequency ratio between the TMD-MR damper and the cable. Based on the theoretical analysis, for the first mode vibration, the TMD-MR damper is most effective when it is located at the mid-span of the cable; the reduction effect increases with the increase of the TMD-MR damping.

- Based on the experimental work on the cable-TMD-MR damper system, to achieve the best effect on the cable vibration reduction, it is recommended that the natural frequency of the TMD-MR damper be close to that of the cable. When the excitation frequency is away from the cable natural frequency, the MR component will contribute mainly by providing an additional damping and the TMD-MR damper should be set in the passive mode. In those non-resonant or small vibration cases, the excitation force is too small to overcome the viscous or friction force and increasing the current of the MR damper will tend to lock the damper's movement and thus deteriorate the damping effects. When the excitation frequency is close to the cable natural frequency, the TMD component will contribute mainly by transferring the vibration energy from the cable to the damper and the MR component will work by providing an additional damping and changing natural frequency of TM-MR damper as well.

Reference

Carlson, J. D. (1994). "The Promise of Controllable Fluids." Proceedings of Actuator 94, H. Borgmann and K. Lenz, Eds., AXON Technologie Consult GmbH, 266-270.

Carlson, J. D. and Weiss, K. D. (1994). " A Growing Attraction to Magnetic Fluids." Machine Design. August, 61-64.

Carlson, J. D., Catanzarite, D. M., and St. Clair, K. A. (1995). "Commercial Magnetorheological Fluid Devices." Proceedings of 5th International Conference on ER Fluids, MR Fluidsand Associated Technolodge. University of Sheffield. UK.

Christenson, R. E., Spencer, B. F. Jr. and Johnson, E. A. (2002) "Experimental Studies on the Smart Damping of Stay Cables." Proccedings of 2002 ASCE Structures Congress, Denver, Colorado, USA

Flamand, O. (1995). "Rain-wind induced vibration of cables." Journal of Wind Engineering and Industrial Aerodynamics, 57, 353 –362

Hikami, Y. (1986). "Rain vibrations of cables in cable-stayed bridges." Journal of Wind Engineering, 27, 17-28 (in Japanese)

Irvine, H.M. and Caughey, T.K. (1974) 'The linear theory of free vibrations of a suspended cable.' Proceedings of Royal Society (London), A341, 299-315.

Irvine, H. M (1978) "Free Vibration of Inclined Cables." Journal of Structural Division, proceedings of the ASCE, Vol. 104, No. ST2, 343-347.

Irvine, H.M. (1981) 'Cable Structure.' MIT Press Series in Structural Mechanics, Cambridge, Massachusetts, and London, England, 1981

Irwin, P.A. (1997). Wind Vibrations of Cables on Cable-Stayed Bridges. Proceedings of ASCE Structures Congress. Vol. 1, April 1997, 383-387.

Johnson, E. A., Spencer, B. F., and Fujino, Y. (1999a) "Semiactive Damping of Stay Cables: A Preliminary Study" Proceedings of 17th International Modal Analysis Conference, Kissimmee, Florida.

Johnson, E. A., Baker, G. A., Spencer, B. F., and Fujino, Y. (1999b) "Mitigating Stay Cable Oscillation Using Semiactive Damping" Proceedings of SPIE, Vol. 3988, Smart Structures and Materials 2000: Smart Systems for Bridges, Structures, and Highway, S. C. Liu, Editor, 207-216

Langsoe H. E., and Larsen, O. D., (1987). "Generating mechanisms for cable stay oscillations at the FARO bridges" Proceeding, International Conference on Cable-stayed Bridges, Bangkok, November 18-20

Li, W. H., Yao, G. Z., Chen, G., Yeo, S. H. and Yap, F. F. (2000). "Testing and Steady State Modeling of a Linear MR Damper under Sinusoidal Loading." Smart Materials and Structures, Vol. 9, 95-102.

Lord Corporation (1999) "Engineering Note for Designing with MR Fluids" http://literature.lord.com/root/other/rheonetic/designing_with_MR_fluids.pdf

Lord Corporation. (2004). http://www.lord.com/Default.aspx?tabid=1127&page=1&docid=684, 04/20/2004

Lou, W. J., Ni, Y. Q., and Ko, J. M. (2000) "Dynamic Properties of a Stay Cable Incorporated with Magnetorheological Fluid Dampers." Advances in Structural Dynamics, J.M. Ko and Y.L. Xu (eds.), Elsevier Science Ltd., Oxford, UK, Vol. II, 1341-1348.

Main, J. A., and, Jones, N. P. (2001). "Evaluation of Viscous Dampers for Stay-cable vibration mitigation" Journal of Bridge Engineering, ASCE, 6(6), 385-397

Main, J. A., and, Jones, N. P. (2002a). "Free vibration of taut cable with attached damper. I: linear viscous damper." Journal of Engineering Mechanics, 128(10), 1062-1071

Main, J. A., and, Jones, N. P. (2002b). "Free vibration of taut cable with attached damper. II: Nonlinear damper." Journal of Engineering Mechanics, 128(10), 1072-1081

Matsumoto, M., Shirashi, N., Shirato, H. (1992). "Rain-wind induced vibration of cables of cable-stayed bridges." J. Wind Engineering and Industrial Aerodynamics, 44, 1992: 2011-2022

Matsumoto, M., Saitoh, T., Kitazawa, M., Shirato, H., and Nishizaki, T.(1995). "Response characteristics of rain-wind induced vibration of stay-cables of cable-stayed bridges." J. Wind Engineering and Industrial Aerodynamics, 57, 323-333

Phelan, R. S., Mehta, K. C., Sarkar, P.P. and Chen, L. (2002). "Investigation of Wind-Rain-Induced Cable-Stay Vibrations on Cable-Stayed Bridges" Final Report, Center for Multidisciplinary Research in Transportation, Texas Tech University, Lubbock, Texas.

Routh, E.J., Dynamics of a system of rigid bodies, Dover Publications, Inc., New York, NY, 1955.

Starossek, U. (1994). "Cable dynamics - A review." IABSE, Structural Engineering International, Vol. 4, No. 3, pp. 171-176.

Tabatabai, H., and Mehrabi, A. B. (1999). "Tuned dampers and cable fillers for suppression of bridge stay cable vibrations." Final report to TRB IDEA program, Construction Technology Laboratories, Inc, Skokie, Illinois

Tabatabai, H., and Mehrabi, A. B. (2000). "Design of Mechanical Viscous Dampers for Stay Cables." Journal of Bridge Engineering, 5(2), 114 – 123

Triantafyllou, M.S.(1984) "The Dynamics of Taut inclined cables." Quarterly Journal of Mechanics and Applied Mathematics, Vol. 27, NO.3, Aug., 1984, pp.421-440

Yang, G. Q. (2001) "Large-Scale Magnetorheological Fluid Damper for Vibration Mitigation: Modeling, Testing and Control." Doctoral Dissertation, University of Notro Dame, Notre Dame, IN

Appendix

Appendix A: Some Experimental Results of Individual MR Dampers

Results of MR RD-1005-3

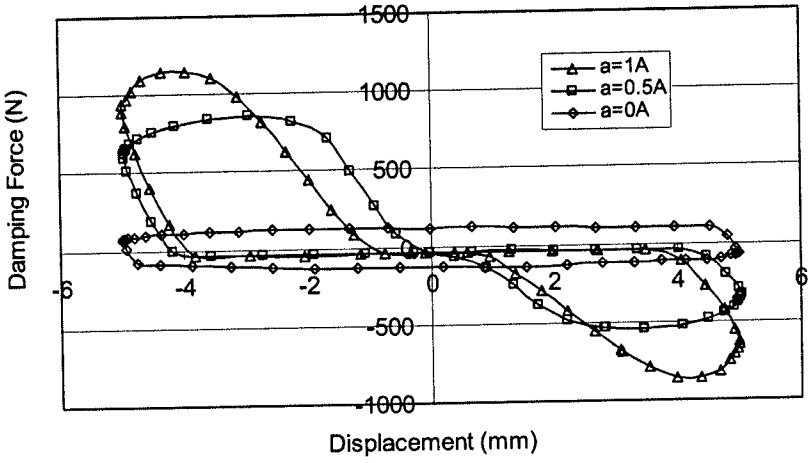

(a)

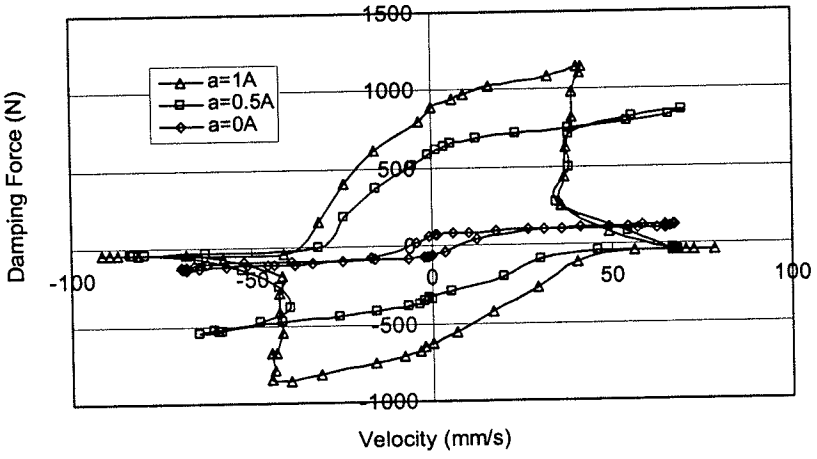

(b)

Fig. A-1: Performance Curve with Different Currents: f=0.5Hz

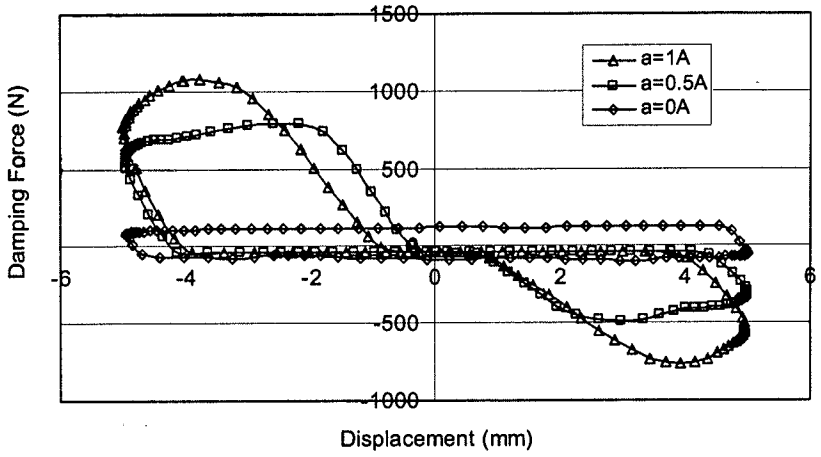

(a)

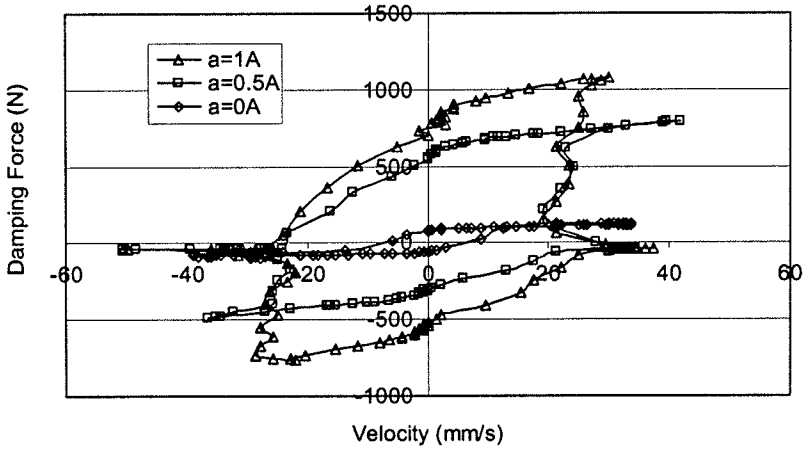

(b)

Fig. A-2: Performance Curve with Different Currents: f=1Hz

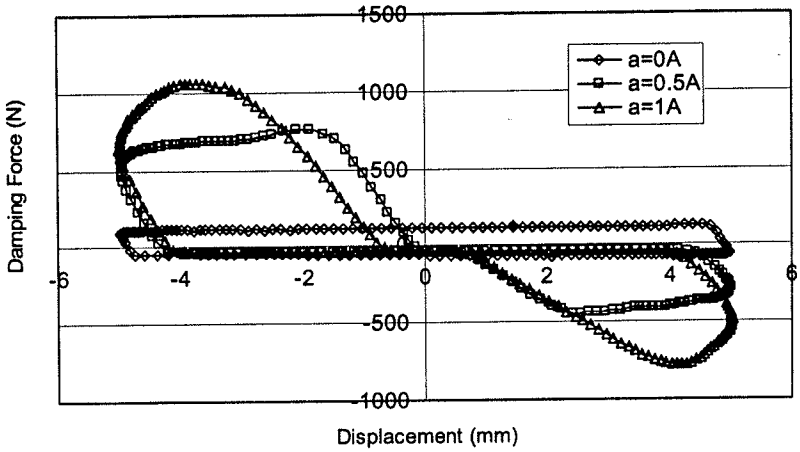

(a)

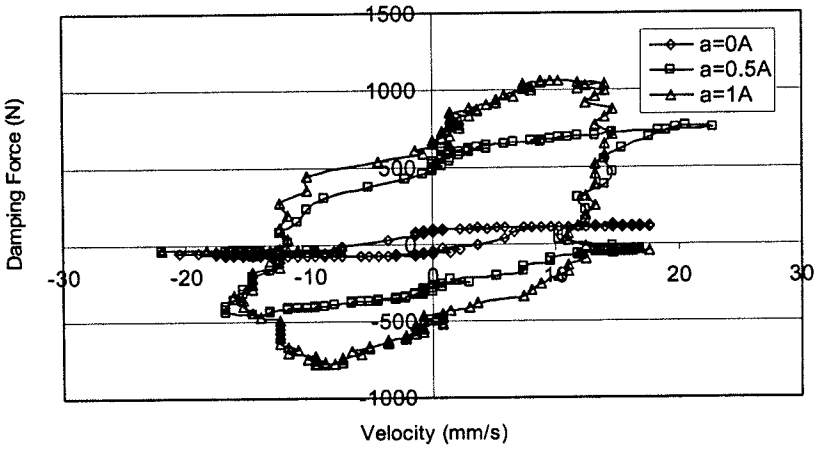

(b)

Fig. A-3: Performance Curve with Different Currents: f=2Hz

Results of MR RD-1097-01

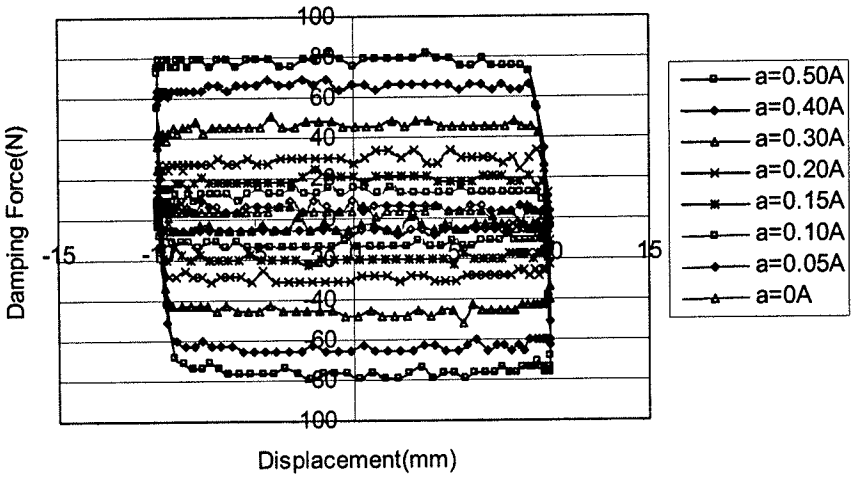

(a)

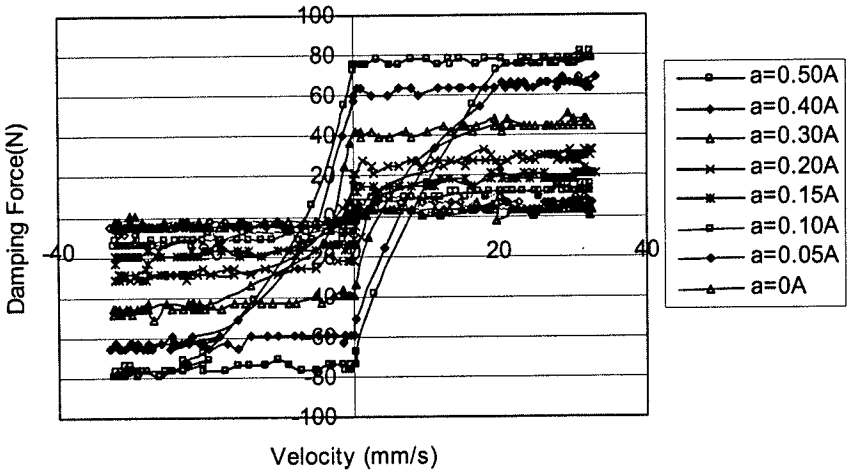

(b)

Fig. A-4: Performance Curve with Different Currents: f=0.5Hz

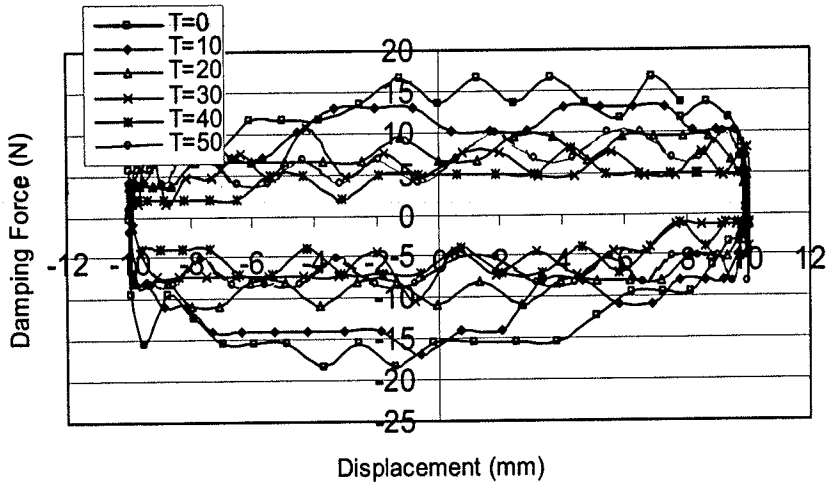

(a)

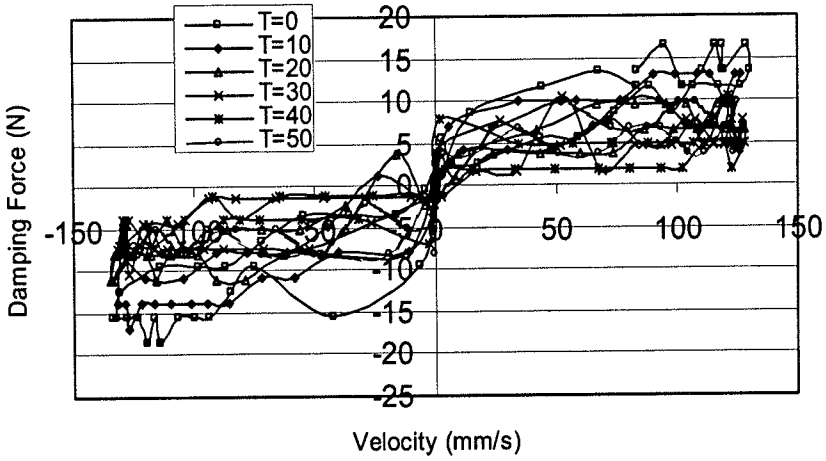

(b)

Fig. A-5: Performance Curve with Different Temperatures: f=2Hz, a=0A

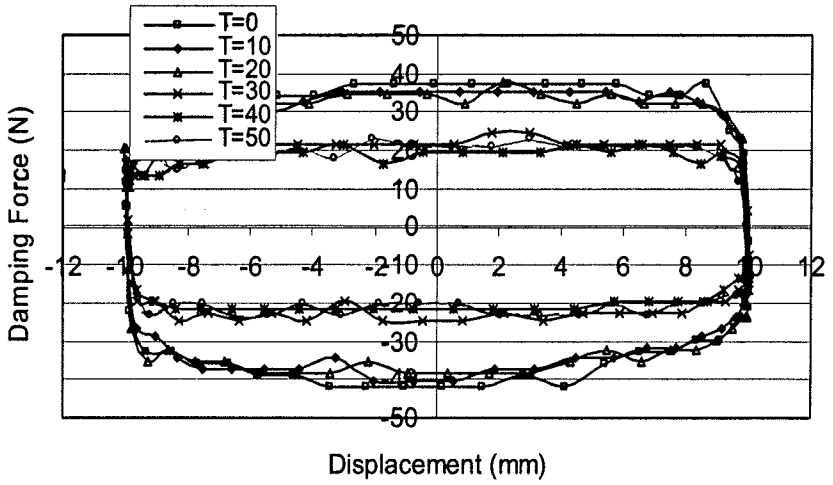

(a)

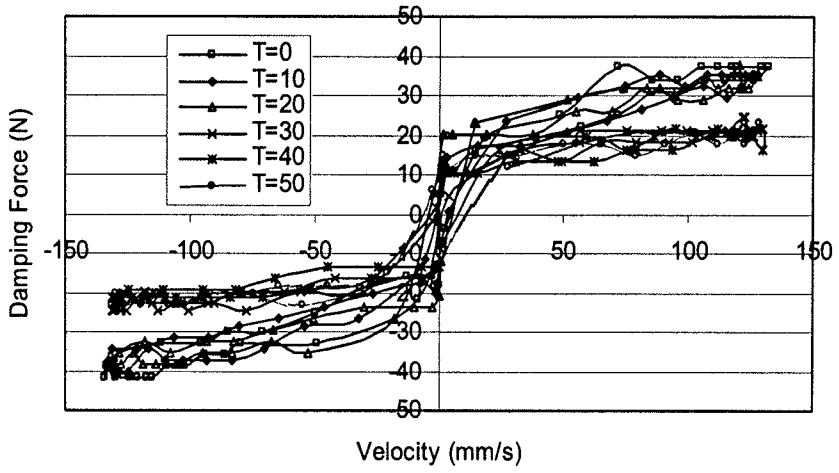

(b)

Fig. A-6: Performance Curve with Different Temperatures: f=2Hz, a=0.20A

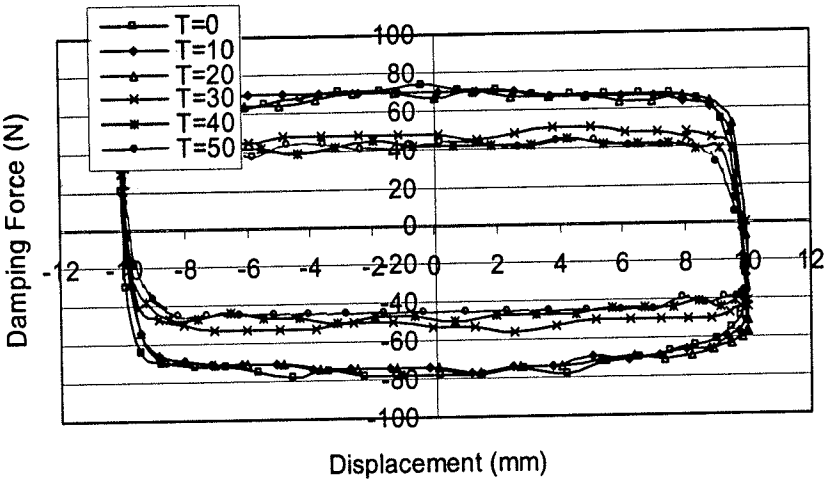

(a)

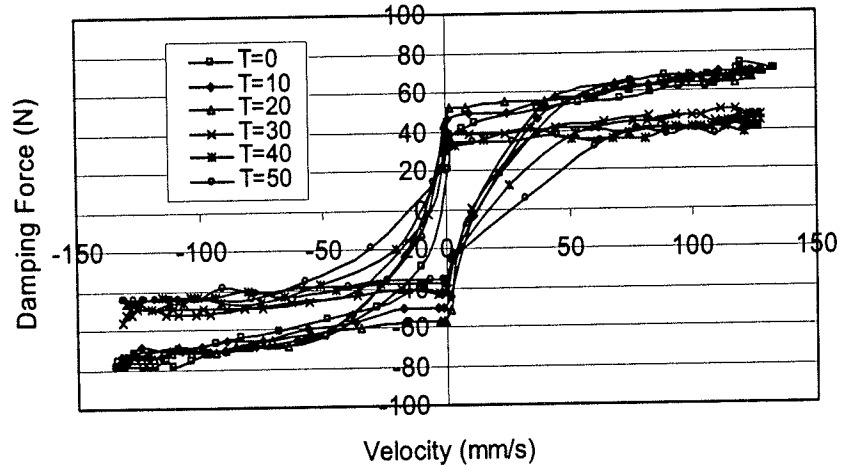

(b)

Fig. A-7: Performance Curve with Different Temperatures: f=2Hz, a=0.40A

Appendix B: Some More Experimental Results of Cable-MR System of Forced Vibration

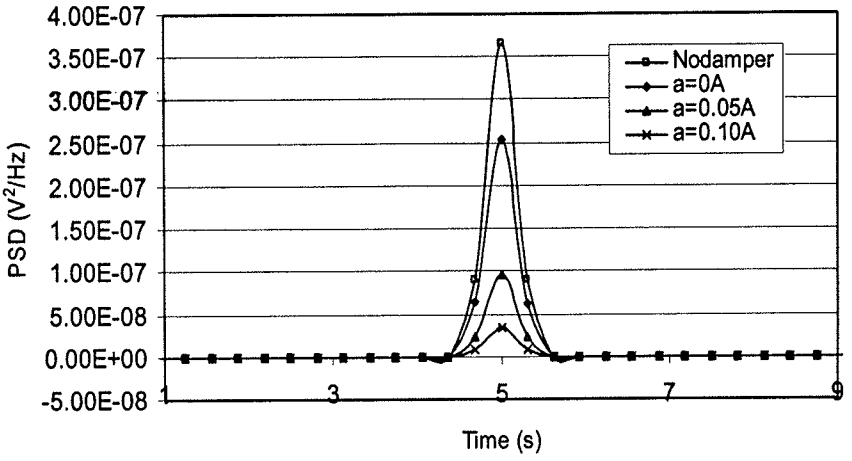

Fig. B-1: Cable Acceleration PSD with 5Hz Sine Wave

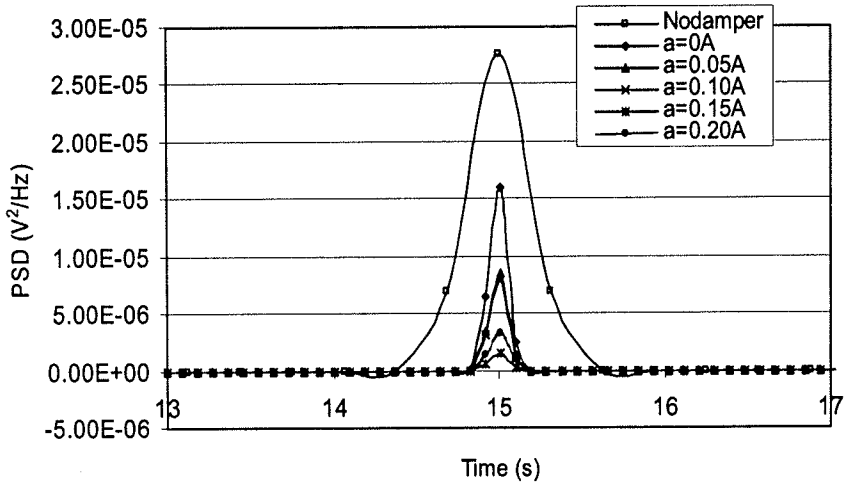

Fig. B-2: Cable Acceleration PSD with 15Hz Sine Wave

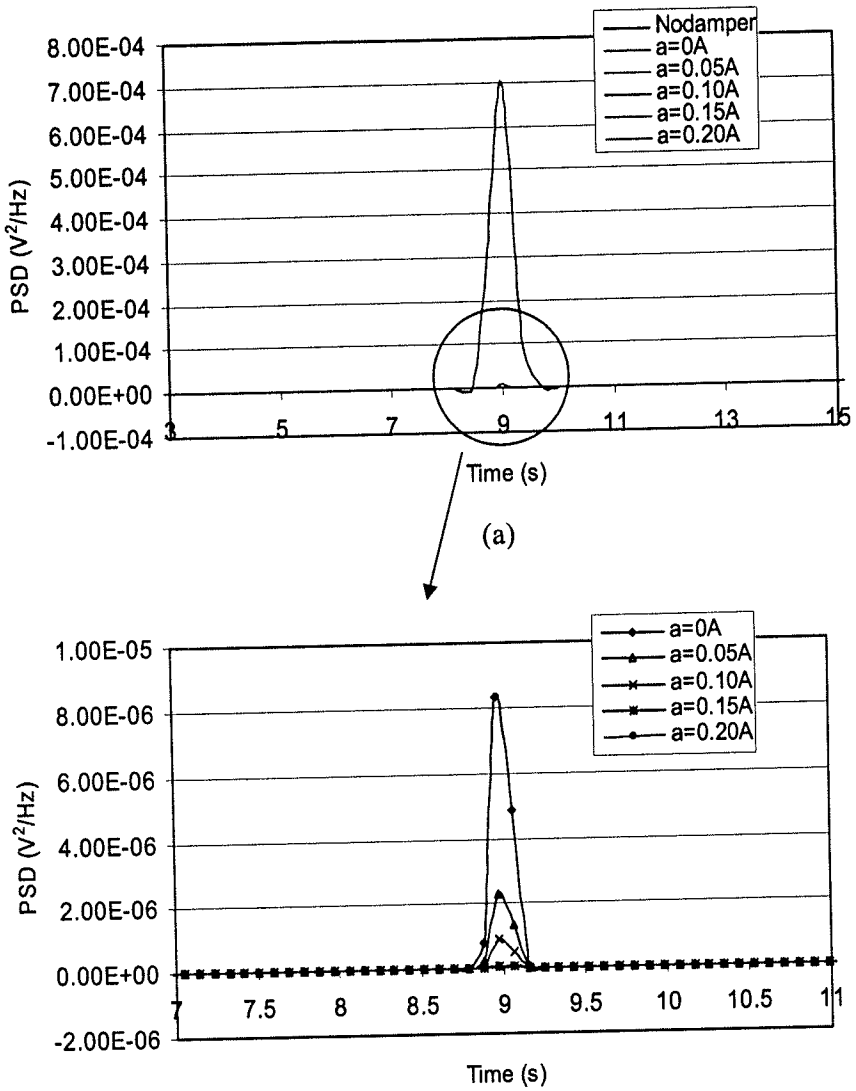

(b) Close Look of (a)

Fig. B-3: Cable Acceleration PSD with 9Hz Sine Wave

Appendix C: Details for Adjustable TMD-MR Damper Design

As stated previously, MR damper design consists of two steps: geometry design and magnetic circuit design. Lord Corporation Engineering Note (1999) provides much information about the design procedure. The main process is summarized and the detailed design and analysis done by the investigation group are provided here for reference.

Geometry Design

Most MR dampers used in civil engineering are pressure driven flow mode though some other types are applied in other areas. Fig. C-1 shows an actual pressure driven flow damper and its magnetic circuit.

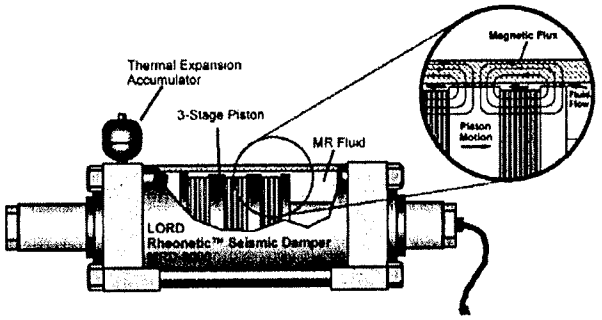

Fig. C-1: Actual Pressure Driven Flow MR Fluid Damper

According to fluid dynamics analysis (Yang 2001), the pressure drop developed in the pressure driven flow mode is assumed as the sum of a viscous component ΔP_η and a field dependent induced yield stress component ΔP_τ. Therefore, the pressure drop can be expressed as:

$$\Delta P = \Delta P_\eta + \Delta P_\tau = \frac{12\eta QL}{g^3 w} + \frac{c\tau_y L}{g} \qquad \text{(C-1)}$$

In Eq. (C-1), Q is the volumetric flow rate while c is a constant mainly determined by the ratio $\Delta P_\tau / \Delta P_\eta$. It is chosen as 2.5 in the TMD-MR system design in the present study.

The minimum active fluid volume V and the dynamic range λ are introduced to get some insight of the parameter variation. The former is the volume of MR fluid exposed to the magnetic field and thus is responsible in providing the desired MR effect. The latter is defined as the ratio between a controllable component and an uncontrollable component. After some simplifications, the following equation can be derived:

$$V = k(\frac{\eta}{\tau_y^2})\lambda W_m \qquad \text{(C-2)}$$

In Eq. (C-2), k is a constant and $V = Lwg$ is the necessary active fluid volume in order to achieve the desired control ratio λ at a required controllable mechanical power level $W_m = Q\Delta P_\tau$. Also, the following equations can be obtained.

$$k = 12/c^2,\ \lambda = \Delta P_\tau / \Delta P_\eta,\ wg^2 = \frac{12}{c}(\frac{\eta}{\tau_y})\lambda Q \qquad \text{(C-3)}$$

Eqs. (C-2) and (C-3) provide geometric constrains for MR devices based on MR fluid properties and the desired ratio or dynamic range. If the required parameters such as the mechanical power level, the desired control ratio, the volumetric flow rate and the material properties are specified, the dimensions of the MR damper can be calculated by using the corresponding equations. Maybe the existing design method can be improved by using output damping force as a required parameter directly, but the discussion of the optimal design method is out of the scope of this investigation.

MR Damper Magnetic Circuit Design

The objective of the magnetic circuit design is to determine necessary amp-turns (NI) to provide a sufficient magnetic field for MR fluid. Therefore, the magnetic circuit design is also important for MR dampers. An optimal design of the magnetic circuit requires maximizing the magnetic field energy in the fluid gap while minimize the energy lost in steel flux conduit and regions of non-working areas. Low carbon steel, which has high magnetic permeability and saturation, is used as a magnetic flux conduit to guide and focus magnetic flux into the fluid gap.

The typical design process for a magnetic circuit is:

(1) Choose a desired yield stress τ_0, and determine the corresponding magnetic induction B_f in the MR fluid from Fig. C-2(a).

(2) Determine the magnetic field intensity H_f in the MR fluid from Fig. C-2(b).

(3) According to the continuity of magnetic induction flux, we have the following equation,

$$\Phi = B_f A_f = B_s A_s \qquad \text{(C-4)}$$

where A_f is the effective pole area including the fringe of magnetic flux and A_s is the steel area. Consequently the magnetic induction B_s in the steel is given by:

$$B_s = \frac{B_f A_f}{A_s} \qquad \text{(C-5)}$$

(4) Determine the magnetic field intensity H_s in the steel, using Fig. C-2(c).

(5) By using Kirchoffs's Law of magnetic circuits, the necessary number of amp-turns (NI) is

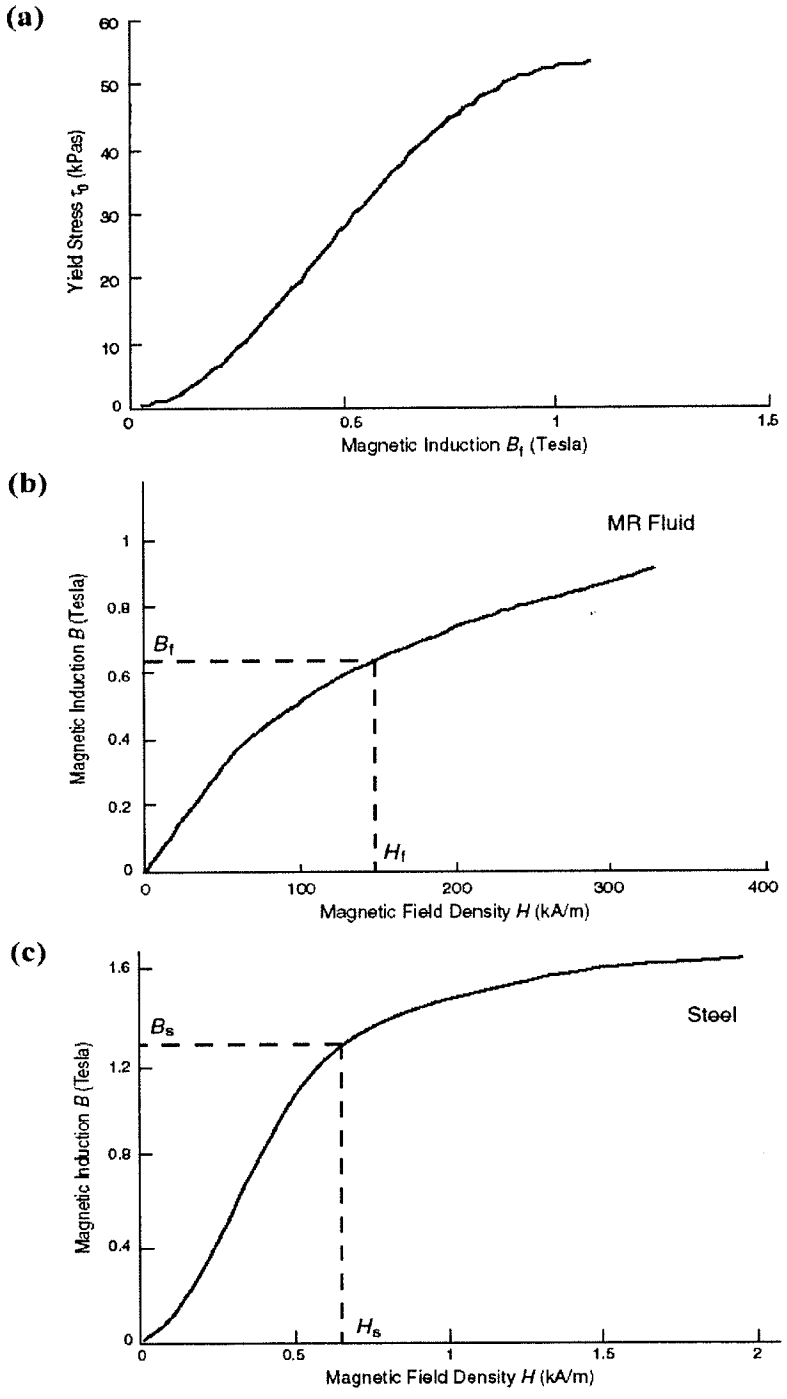

Fig. C-2: Magnetic Design Information (Courtesy of Lord Corporation)

$$NI = \sum_i H_i L_i = H_f g + H_s L \tag{C-6}$$

Other effects should also be considered during the circuit design process, such as non-linear magnetic properties of the MR fluid and steel, possible losses at the junctions and boundaries, limits on voltage, current, and inductance, possible inclusion of permanent magnets for fail-safe operation, and eddy currents. However, those factors are out of the scope of this study.

Pressure Driven Flow Damper Design

Based on the cable experimental data obtained previously and the fluid material property of MRF-336AG provided by Lord Corporation, we define the required parameters to match the cable as,

Table C-1: Assumed Design Parameter

Parameter	Value	Parameter	Value
Maximum force	~50 N	Minimum force	~5 N
Dynamic range	10	Outer Diameter (d_1)	20 mm
Yield Stress	45000 pa	Viscosity	4~8 $pa \cdot s$
Magnetic induction	0.75 T	Cable frequency	1~10 Hz

Assume that the active pressure drop area A_p is about 60 mm^2, the demanded pressure drop is determined as,

$$\Delta P_\tau = 50N/60mm^2 \approx 800000pa \tag{C-7}$$

Assume the cable frequency is about 4 Hz, and the amplitude of cable vibration is about 1 mm, then the maximum volumetric flow rate is about,

$$Q_{\max} = 2\pi faA_p = 2\times 3.14159\times 4\times 1\times 60 \approx 1500mm^3/s \tag{C-8}$$

The minimum active fluid volume V can be calculated as,

$$V = k(\frac{\eta}{\tau_y^2})\lambda\Delta P_\tau Q_{\max} = \frac{12}{2.5^2}\times\left(\frac{4}{45000^2}\right)\times 10\times 800000\times 1500 = 45.5mm^3 \tag{C-9}$$

Using Eq. (C-3), we get,

$$wg^2 = \frac{12}{c} \times \left(\frac{\eta}{\tau_y} \right) \times \lambda \times Q_{\max} = \frac{12}{2.5} \times \left(\frac{4}{45000} \right) \times 10 \times 1500 = 6.4 \qquad \text{(C-10)}$$

Followed the procedure explained earlier, we obtain,

$$g = 0.36mm, L = 2.5mm \qquad \text{(C-11)}$$

From Fig. C-3, the magnetic field intensity is 175 kAmp/m for the assumed value $\tau_y = 45000pa$. According to Eqs. (C-5) and (C-6), we can finally determine that the necessary number of amp-turns (NI) is about 90. Consequently, if the maximum current provided to the MR damper is 0.5 ampere, then the turn number can be determined as 180.

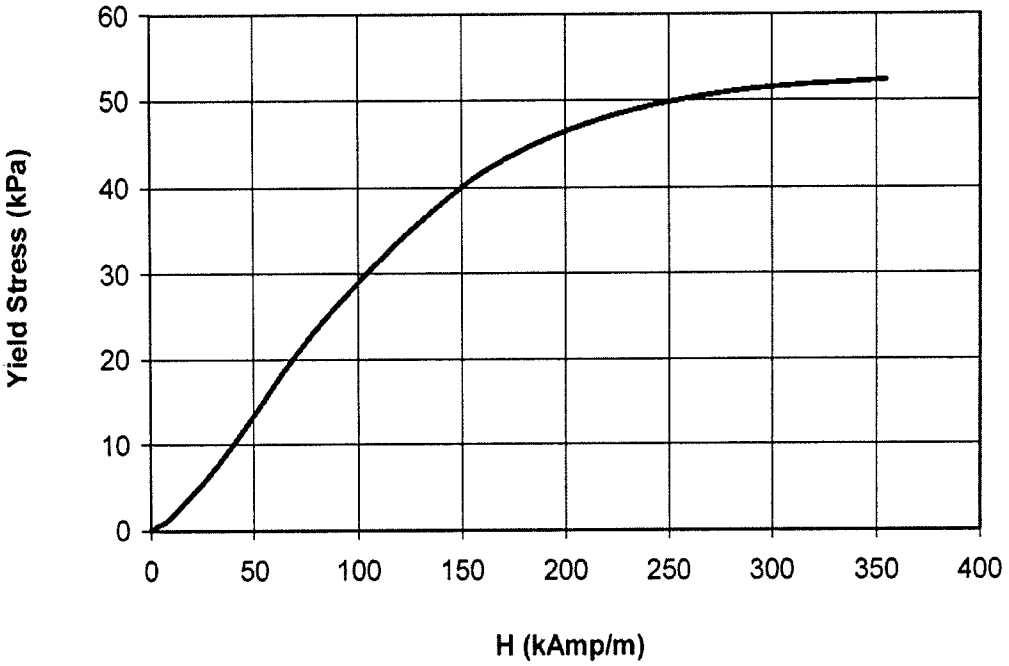

Fig. C-3: Yield Stress Versus Magnetic Field Intensity of MRF-33AG
(Courtesy of www.lord.com)

Following the procedure explained above, all the parameters for the geometry and magnetic circuit designs can be obtained. Nevertheless, if we want to have an optimal design, we need to know the relationships between the variations of the design parameters and those assumed parameters in Table C-1. Table C-2 gives the changing rule of these parameters (dependency of the variables). In this table, f is the corresponding cable vibration frequency and d is the interval for magnetic coil winding. All the other variables have been defined earlier. In the table below, the symbols "↓",

"↔" and "↑" mean that the corresponding value will decrease, remain unchanged, and increase, respectively.

Table C-2: Variety Rule for MR Design Parameter

	V	g	L	N	F_τ	F_η	f
$\Delta P_\tau \uparrow$	↓	↔	↓	↔	↓	↓	↔
$Q_{max} \uparrow$	↓	↓	↓	↓	↔	↔	↓
$\lambda \uparrow$	↓	↓	↓	↓	↔	↑	↔
$d_1 \uparrow$	↔	↑	↑	↑	↓	↓	↑
$\tau_y \uparrow$	↑	↑	↑	↑	↔	↔	↔
$\eta \uparrow$	↓	↓	↓	↓	↔	↔	↓
$d \uparrow$	↓	↔	↔	↓	↔	↔	↔
$t \uparrow$	↔	↓	↓	↓	↑	↑	↓
$r_4 \uparrow$	↔	↔	↔	↑	↑	↑	↓

Appendix D: Theoretical Solution of Cable-TMD-MR System

Cable Dynamics

There are a large amount papers in the literature discussing cable static and dynamic problems. By 1788, Lagrange and others had obtained solutions of varying degrees of completeness for the vibrations of an inextensible, massless string with hung on weights and fixed ends. These supplementary weights need a discretization model of the cable continuum. In 1820, Poison proposed a set of general partial differential equations of the motion of a cable element under the action of a general force system. However, apart from Lagrange's work on the equivalent discrete system, solutions for the sagging cable were unknown at that time (Starossek, 1994). Routh (1955) gave exact solutions for an inextensible sagging cable. Before 1970s, there was no explanation on the obvious discrepancy between the theories of an inextensible sagging cable and a taut cable. Irvine and Caughey (1974) revealed an extensive comprehension of the linear theory of free vibrations of a rigidly supported horizontal cable with a ratio of sag to span from approximately 1:8 or less. With a parameter representing the geometry and elasticity of the cable under consideration, they pointed out that if the elasticity is considered, the discrepancy could be explained. Later on, Irvine extended the theory to inclined cables by neglecting the weight component parallel to the cable chord (Irvine 1978). Triantafyllou (1984) derived a more precise asymptotic solution for small-sag, inclined, elastic cables. He demonstrated that inclined cables have different properties so that the horizontal cable results can't be simply extended to inclined cables. Nevertheless, validity of Irvine's theory was confirmed for a wide range of parameters.

Based on the previous extensive investigation on cable dynamics, Main and Jones (2002a, 2002b) discussed a horizontal cable with a viscous damper. In their investigation, they assumed that the tension in the cable is large compared to its weight, bending stiffness and intrinsic damping of cable are negligible, and deflections are small. Following their procedure, some theoretical discussions will also be carried out in this investigation.

Theoretical Derivation

As stated previously, the equation of motion of the cable-TMD-MR system can be expressed as:

$$T\frac{\partial^2 v_k(x_k,t)}{\partial x_k^2} = m\frac{\partial^2 v_k(x_k,t)}{\partial t^2} \qquad \text{(D-1)}$$

Traditionally, variable separation method is used to solve Eq. (D-1), meaning that the solution is assumed to have the following form:

$$v_k(x_k,\tau) = V_k(x_k)e^{s\tau} \tag{D-2}$$

where s is a dimensionless eigenvalue that is complex in general, while V_k is the mode shape of the cable vibration. Substituting Eq. (D-2) into Eq. (D-1) yields the following ordinary differential equation:

$$\frac{d^2V_k(x_k)}{dx_k^2} = (\frac{\pi s}{L})^2 V_k \tag{D-3}$$

From the boundary conditions, we have,

$$v_k(0,\tau) = 0\ ,\ k = 1,2 \tag{D-4}$$

From the continuity of the cable at the conjunction point of the two segments, we have,

$$v_1(l_1,\tau) = v_2(l_2,\tau) = \gamma(\tau) \tag{D-5}$$

which means though the amplitude of the damper γ varies with time, the cable deflection is continuous for the two segments.

With these boundary and continuity conditions, the cable displacement can be expressed as,

$$v_k(x_k,\tau) = \gamma(\tau)\frac{\sinh(\pi s x_k / L)}{\sinh(\pi s l_k / L)} \tag{D-6}$$

Also, considering the vertical equilibrium condition at the hang-on point of the TMD-MR damper, we have,

$$T(-\frac{\partial v_1}{\partial x_1}\bigg|_{x_1=l_1} - \frac{\partial v_2}{\partial x_2}\bigg|_{x_2=l_2}) = K(v_1\big|_{x_1=l_1} - v_d) + C(\frac{dv_1}{dt}\bigg|_{x_1=l_1} - \frac{dv_d}{dt}) \tag{D-7}$$

On the other hand, from the equilibrium of the damper system itself, we have,

$$K(v_1\big|_{x_1=l_1} - v_d) + C(\frac{dv_1}{dt}\bigg|_{x_1=l_1} - \frac{dv_d}{dt}) - M\frac{d^2v_d}{dt^2} = 0 \tag{D-8}$$

where, v_d is the vertical displacement of the TMD-MR damper system and K, C and M are stiffness, damping coefficient and mass of the damper system, respectively.

Since only the steady-state response is taken into account, it is reasonable to assume that the damper system has the same vibration pattern as the cable vibration at the place where it hangs on. According to this assumption, the displacement of the damper system can be expressed as,

$$v_d = \beta\gamma(\tau) \tag{D-9}$$

where the constant β is the amplitude ratio between the vibration of the damper and corresponding cable point.

From Eq. (D-8), and also denote $K = M\omega_d^2$ and $C = 2M\omega_d\xi$, we can express β as:

$$\beta = \frac{1+2\xi\rho s}{1+2\xi\rho s+\rho^2 s^2} \tag{D-10}$$

in which, ω_d is the natural frequency of the damper, ξ is the damping ratio, and $\rho = \frac{\omega_c}{\omega_d}$ can be viewed as a ratio between the cable frequency and the damper frequency.

Substituting β into Eq. (D-9) and then into Eq. (D-7), we have:

$$\coth(\frac{\pi s l_1}{L}) + \coth(\frac{\pi s l_2}{L}) + \frac{\pi s}{L}\frac{M}{m}\frac{1+2\xi\rho s}{1+2\xi\rho s+\rho^2 s^2} = 0 \tag{D-11}$$

From this transcendental equation, s can be obtained if the cable and damper parameters are specified.

Usually, the complex value s can be expressed as the sum of its real part and its imaginary part as:

$$s_i = \sigma_i + j\varphi_i \tag{D-12}$$

where the subscript i corresponding to the ith mode. σ_i and φ_i are both real values, and $j = \sqrt{-1}$. The system damping is defined as,

$$\zeta_i = (\frac{\varphi_i^2}{\sigma_i^2}+1)^{-1/2} \tag{D-13}$$

Treating the real and imaginary parts of Eq. (D-11) separately, we can obtain:

$$\begin{aligned}
&\frac{\sinh(2\pi\sigma_i l_1/L)}{\cosh(2\pi\sigma_i l_1/L)-\cos(2\pi\varphi_i l_1/L)} + \frac{\sinh(2\pi\sigma_i l_2/L)}{\cosh(2\pi\sigma_i l_2/L)-\cos(2\pi\varphi_i l_2/L)} + \\
&\frac{\pi M}{Lm}\Big(\frac{\sigma_i+\sigma_i^2(4\xi\rho)+\sigma_i^3(\rho^2+4\xi^2\rho^2)+\varphi_i^2\sigma_i(\rho^2+4\xi^2\rho^2)}{(1+2\xi\rho\sigma_i+\rho^2\sigma_i^2-\rho^2\varphi_i^2)^2+(2\xi\rho\varphi_i+2\rho^2\varphi_i\sigma_i)^2} \\
&+\frac{\sigma_i^4(2\xi\rho^3)+\varphi_i^2\sigma_i^2(4\xi\rho^3)+\varphi_i^4(2\xi\rho^3)}{(1+2\xi\rho\sigma_i+\rho^2\sigma_i^2-\rho^2\varphi_i^2)^2+(2\xi\rho\varphi_i+2\rho^2\varphi_i\sigma_i)^2}\Big) = 0
\end{aligned} \tag{D-14}$$

$$\frac{-2\sin(2\pi\varphi_i l_1/L)\cosh(2\pi\sigma_i l_1/L)-2\sin(2\pi\varphi_i l_2/L)\cosh(2\pi\sigma_i l_2/L)+2\sin(2\pi\varphi_i)}{(\cosh(2\pi\sigma_i l_1/L)-\cos(2\pi\varphi_i l_1/L))(\cosh(2\pi\sigma_i l_2/L)-\cos(2\pi\varphi_i l_2/L))}+$$

$$\frac{\pi M}{Lm}\frac{\varphi_i+\varphi_i\sigma_i(4\xi\rho)+\varphi_i{\sigma_i}^3(4\xi\rho-4\xi\rho^3)+{\varphi_i}^2{\sigma_i}^2(4\xi^2\rho^2-\rho^2)+{\varphi_i}^3(4\xi^2\rho^2-\rho^2)}{(1+2\xi\rho\sigma_i+\rho^2{\sigma_i}^2-\rho^2{\varphi_i}^2)^2+(2\xi\rho\varphi_i+2\rho^2\varphi_i\sigma_i)^2}=0 \qquad \text{(D-15)}$$

These equations are solved numerically and some of the results have been discussed earlier in the text.

Appendix E: Some More Experimental Results of Cable-TMD-MR System

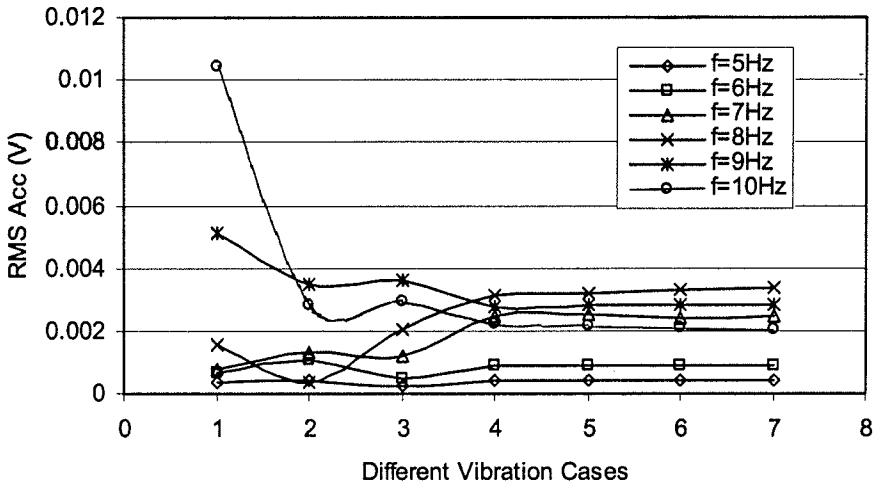

(a)

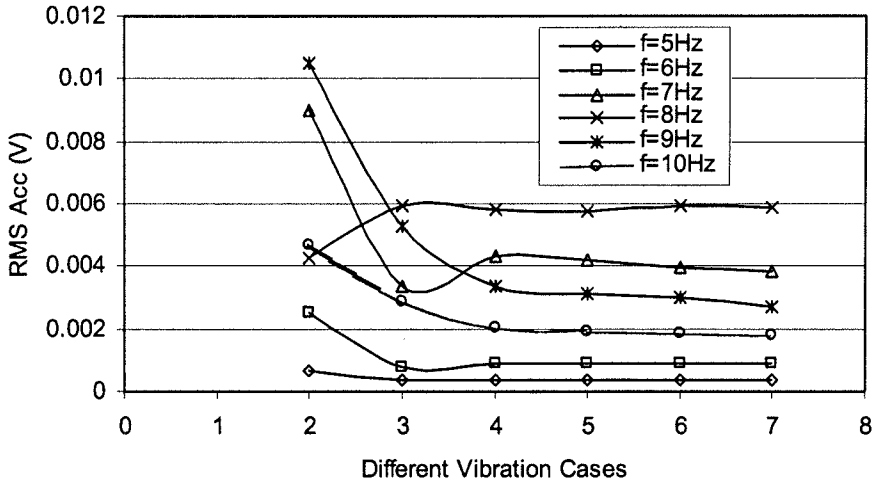

(b)

Fig. E-1: RMS Acceleration of Cable-TMD-MR System under Different Experimental Setup (a) Cable, (b) TMD-MR